Early Afterdepolarizations In Cardiac Myocytes: Mechanism and Rate Dependence

Jinglin Zeng and Yoram Rudy
Cardiac Bioelectricity Research and Training Center, Department of Biomedical Engineering, Case Western Reserve University, Cleveland, Ohio 44106-7207 USA

ABSTRACT A model of the cardiac ventricular action potential that accounts for dynamic changes in ionic concentrations was used to study the mechanism, characteristics, and rate dependence of early afterdepolarizations (EADs). A simulation approach to the study of the effects of pharmacological agents on cellular processes was introduced. The simulation results are qualitatively consistent with experimental observations and help resolve contradictory conclusions in the literature regarding the mechanism of EADs. Our results demonstrate that: 1) the L-type calcium current, I_{Ca}, is necessary as a depolarizing charge carrier during an EAD; 2) recovery and reactivation of I_{Ca} is the mechanism of EAD formation, independent of the intervention used to induce the EADs (cesium, Bay K 8644, or isoproterenol were used in our simulations, following similar published experimental protocols); 3) high $[Ca^{2+}]_i$ is not required for EADs to develop and calcium release by the sarcoplasmic reticulum does not occur during the EAD; 4) although the primary mechanism of EAD formation is recovery of I_{Ca}, other plateau currents can modulate EAD formation by affecting the balance of currents during a conditional phase before the EAD take-off; and 5) EADs are present at drive cycle lengths longer than 1000 ms. Because of the very long activation time constant of the delayed rectifier potassium current, I_K, the activation gate of I_K does not deactivate completely between consecutive stimuli at fast rates (drive cycle length < 1000 ms). As a result, I_K plays a key role in determining the rate dependence of EADs.

INTRODUCTION

An early afterdepolarization (EAD) is defined (Cranefield and Aronson, 1988) as a depolarizing afterpotential that begins before the completion of repolarization of an action potential. It is believed that EADs may contribute to the polymorphic ventricular tachyarrhythmias in patients with the long QT syndrome that manifests as Torsade de Pointes in the electrocardiogram (Hiraska et al., 1992; January and Moscucci, 1992). EAD-induced arrhythmias are bradycardia-related and are associated with slow pacing or a long pause (Cranefield and Aronson, 1988; Damiano and Rosen, 1984; Rosen, 1990).

EADs are divided into two types according to the phase of the action potential during which the EAD occurs (Cranefield and Aronson, 1988). We are interested in EADs that develop at plateau potentials. EADs were induced experimentally in several studies by exposure to different pharmacological interventions. However, as summarized below and presented in Fig. 1, because of experimental limitations such as lack of specificity of drug actions and inability to measure directly certain ionic currents and concentration changes (e.g., the calcium transient), conclusions regarding the mechanism of EADs are conflicting and not conclusive.

Exposing the ferret ventricular muscle to cesium, Marban et al. (1986) found that EADs induced by cesium (Fig. 1*A*) were neither abolished by administration of ryanodine, an inhibitor of Ca^{2+} release from the sarcoplasmic reticulum (SR), nor by loading the cell with BAPTA (a calcium chelator). They concluded that the formation of EADs does not require elevated intracellular free Ca^{2+} or calcium release from the SR. Instead, they suggested that EAD generation involves Ca^{2+} entry through the sarcolemma L-type channels.

January and his colleagues (January et al., 1988; January and Riddle, 1989) studied the mechanism of EADs induced by Bay K 8644 in sheep and canine cardiac Purkinje fibers (Fig. 1*B*). Two-pulse and two-step voltage clamp protocols were used in their studies. On the basis of their observations, they suggested that induction of EADs required two processes: 1) prolongation of the action potential plateau and 2) recovery of the Ca^{2+} current through the L-type channels to carry the depolarizing charge for EAD formation. Their later experimental and mathematical modeling studies further supported the central role of the L-type calcium window current in EAD development (Hirano et al., 1992; January et al., 1991; Shorofsky and January, 1992).

Contrary to the L-type calcium current hypothesis presented above, Priori and Corr (1990) proposed that EADs and delayed afterdepolarizations (DADs) shared the same mechanism (Fig. 1*C*). With the administration of isoproterenol, both EADs and DADs were induced. Both could be abolished by ryanodine, by lowering extracellular sodium concentration or by benzamil (a blocker of the sodium-calcium exchange current, I_{NaCa}). Therefore, they concluded that a transient inward current (possibly I_{NaCa}), activated by calcium release from the SR, carried the depolarizing charge for both EADs and DADs.

In this paper, we use a recently developed mathematical model of the cardiac ventricular action potential (the L-R model) (Luo and Rudy, 1994a, b) to study the mechanism of EADs. We take advantage of the ability to manipulate and

Received for publication 7 March 1994 and in final form 15 November 1994.
Address reprint requests to Dr. Yoram Rudy, Department of Biomedical Engineering, Case Western Reserve University, Wickenden Bldg., Room 505, Cleveland, OH 44106-7207. Tel.: 216-368-4051; Fax: 216-368-4969; E-mail: yxr@po.cwru.edu.

0006-3495/95/03/949/16 $2.00

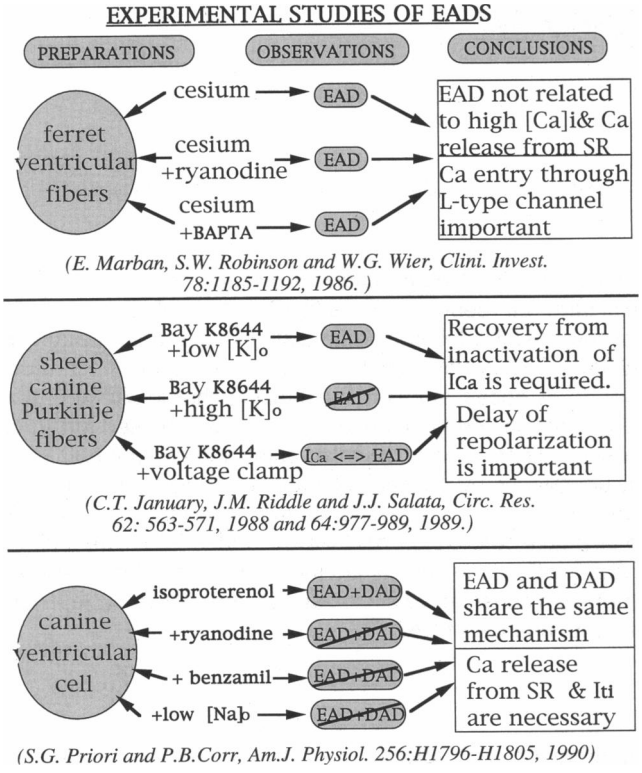

FIGURE 1 Schematic description of three experimental studies of EADs. (*A*) Marban et al [43]. EADs were induced when ventricular fibers were exposed to CsCl and then returned to normal Tyrode solution. Addition of ryanodine or BAPTA did not remove EADs. They concluded that high $[Ca^{2+}]_i$ is not required for EAD formation whereas calcium entry through L-type channels plays an important role. (*B*) January et al [29,30]. In the presence of Bay K 8644, EADs were induced at 3.5 mM $[K^+]_o$ but not at 5.0 mM $[K^+]_o$. On the basis of two-step and two-pulse voltage clamp protocols, they concluded that recovery of L-type channels from inactivation is important for EAD development. (*C*) Priori and Corr [52]. EADs as well as DADs were induced by isoproterenol when the single cell was paced at 1–2 Hz. Both were removed by lowering $[Na^+]_o$ to 40 mM or adding ryanodine or by application of benzamil. They concluded that EADs and DADs share the same mechanism that involves spontaneous Ca^{2+} release by the SR that activates a transient inward current to depolarize the membrane.

study the behavior of individual ionic processes in the mathematical model of the complex and highly interactive cellular system. The effects of cesium, isoproterenol, and Bay K 8644 that were used in the above experiments to induce EADs are simulated in an attempt to resolve the controversy regarding the mechanism underlying EAD formation. In addition, we study the rate dependence of EAD generation and investigate its ionic channel mechanism. These studies were presented, in part, in an abstract form (Zeng and Rudy, 1994a, b).

SIMULATION METHODS

To study the mechanism of EADs, the effects of cesium, Bay K 8644, and isoproterenol, which are known to induce EADs experimentally, are simulated by using the L-R model (Luo and Rudy, 1994a, b). In this model, the guinea pig type of ventricular action potential is numerically constructed on the basis of experimental data. Included in the model are the membrane ionic channel currents, represented mathematically by a Hodgkin-Huxley type of formalism, as well as ionic pumps and exchangers. In addition, processes that regulate ionic concentration changes, especially dynamic changes of intracellular calcium concentration, are also introduced. A diagram of the cell model is provided in Fig. 2. A detailed table of equations governing the model is provided in Luo and Rudy (1994a).

Although the simulations presented here are based on the L-R model, minor adjustments are introduced for the purpose of the particular simulations conducted in this study. It is well known that release of calcium stored in the SR can be triggered by the process of calcium-induced calcium release (CICR) (Fabiato, 1983, 1985). In the model (Luo and Rudy, 1994a), CICR occurs if total $[Ca^{2+}]_i$ (i.e., free plus buffered) increases by more than 0.18 μM in the first 2 ms of the action potential. After a delay of 3–9 ms from the beginning of a stimulus that generates an action potential, free cytoplasmic $[Ca^{2+}]_i$ begins to increase quickly as a result of SR release and reaches its peak value in an additional 8–19 ms (Cleeman and Morad, 1991). During this process, the distribution of free calcium ions in the myoplasm is relatively homogeneous (Takamatsu and Weir, 1989). In the L-R model, this peak is reached 10 ms after the junctional SR (JSR) begins to release its stored calcium. In our simulations, this interval is prolonged to 15 ms (within the 8–19 ms range) by increasing the activation and deactivation time constants of SR calcium release channels from 2 to 3.5 ms. This slower kinetics approximates more accurately the experimental recordings of the time course of the calcium transient (Cleeman and Morad, 1991). We also adjust the maximal rate constant of calcium release from the JSR from 60 to 38 ms^{-1} to obtain a peak Ca^{2+} transient value of 1.0 μM during a normal action potential, as reported experimentally (Leblanc and Hume, 1990).

Calcium can also be released from the JSR spontaneously when the cell is calcium overloaded (Stern et al., 1988). This property is incorporated in the L-R model (Luo and Rudy, 1994a). Heterogeneous calcium distribution in the myoplasm is observed during the spontaneous release process (Grouselle et al., 1991) and the average calcium transient reaches its peak later compared with the calcium transient generated by the CICR process. In the L-R model, all SR release sites are lumped into a single location. To reflect the longer time course of the average calcium transient during spontaneous calcium release, we increase the release channel activation and deactivation time constants from 2 to 6 ms under these conditions. The maximal rate constant is decreased from 4 to 3 ms^{-1}.

In several of our simulations, the cells were paced relatively fast for extended periods of time. Therefore, an extracellular cleft is added to the L-R model to take into account the possibility of ion accumulation in the cleft.

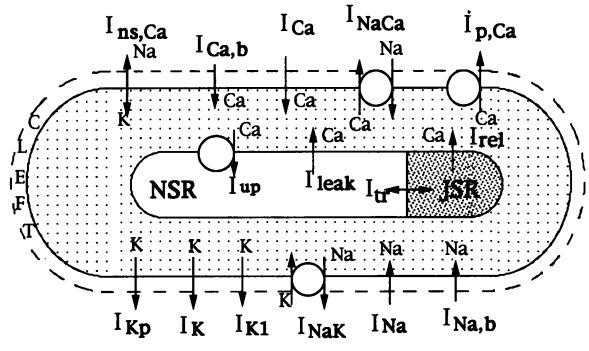

FIGURE 2 Schematic diagram of the L-R single ventricular cell model. I_{Na}, fast sodium current; I_{Ca}, calcium current through L-type calcium channel; I_K, delayed rectifier potassium current; I_{K1}, inward rectifier potassium current; I_{Kp}, plateau potassium current; I_{NaK}, sodium-potassium pump current; I_{NaCa}, sodium-calcium exchange current; $I_{p,Ca}$, calcium pump in the sarcolemma; $I_{Na,b}$, sodium background current; $I_{Ca,b}$, calcium background current; $I_{ns,Ca}$, nonspecific calcium-activated current; I_{up}, calcium uptake from myoplasm to network sarcoplasmic reticulum (NSR); I_{rel}, calcium release from JSR; I_{leak}, calcium leakage from NSR to myoplasm; I_{tr}, calcium translocation from NSR to JSR. Dotted areas indicate presence of calcium buffers. For details, see [41].

Following Rasmusson et al. (1990), we compute the concentration change of ions in the cleft as the balance of two processes, transmembrane ionic current flow and diffusion between the cleft and the bulk medium. A diffusion time constant of 1000 ms was used. Details are provided in Rasmusson et al. (1990).

As mentioned above, the effects of cesium, Bay K 8644, and isoproterenol were simulated to induce EADs in our theoretical studies. The effects of these three drugs and their representation in our simulated protocols are discussed below.

Cesium

Cesium is known to depolarize the resting potential and flatten the plateau of the action potential (Isenberg, 1976). The pacemaker current, I_f, can be blocked by Cs^+ at very low Cs^+ concentrations (down to 0.1 mM) (Isenberg, 1976). I_K and I_{K1} can also be blocked by extracellular Cs^+ (Harvey and Ten Eick, 1989; Meier and Kalzung, 1981). However, high Cs^+ concentration (5 mM) is needed to reduce these two currents. The Cs^+ block of K^+ currents is both voltage and concentration dependent (Meier and Katzung, 1981; Tourneur et al., 1987). To simulate these effects, we introduce a voltage- and concentration-dependent gate, δ_{Cs}, to account for the Cs^+ modulation of the I_K and I_{K1} conductances in the L-R model. To fit the experimental recordings (Meier and Katzung, 1981; Tourneur et al., 1987), δ_{Cs} is expressed as

$$\delta_{Cs} = 1/(1 + \exp((V - V_{1/2})/K_{Cs})) \quad (1)$$

where V is the membrane potential, K_{Cs} is -16 mV, and $V_{1/2}$ is a concentration-dependent parameter. At 5 and 10 mM Cs^+, $V_{1/2}$ is set to -95 and -40 mV, respectively.

Bay K 8644

Bay K 8644 can be divided into two types according to its optical isomers: the (+) isomer of Bay K 8644, which shows properties of a calcium L-type channel antagonist, and the (−) isomer of Bay K 8644, which is primarily an L-type Ca^{2+} channel agonist (Frankowiak et al., 1985). In this study, we are interested in the (−) isomer of Bay K 8644 at 1 μM concentration. Bay K 8644 is a 1,4-dihydropyridine that can increase the microscopic Ca^{2+} currents by prolonging the mean open time of single L-type channels (Hess et al., 1984). At a concentration of 1 μM, the enhancement of the L-type Ca^{2+} channel current reaches its maximum. It is generally observed that the steady state activation and inactivation curves are shifted toward hyperpolarization potentials by Bay K 8644 and the time constants for both activation and inactivation are accelerated in the presence of Bay K 8644. There are many published studies describing the effects of Bay K 8644 on the kinetics of the L-type Ca^{2+} channel (Hadley and Lederer, 1992; Markwardt and Nilius, 1988; Sanguinetti et al., 1986). Because of species differences and differences in the experimental protocols, the results of the different studies are not in complete agreement (Sanguinetti et al., 1986; Markwardt and Nileus, 1988; Kass, 1987; Hadley and Lederer, 1992, Tiaho et al., 1990). Our simulations of Bay K 8644 effects on the L-type current mostly follow the measurements by January et al. (1988) as our objective is to simulate their experimental protocols. In the presence of 1 μM Bay K 8644, the maximal permeability of I_{Ca} is enhanced threefold. The $V_{1/2}$ of the activation curve of the L-type channel is shifted from -10 to -17.5 mV to reflect the measured 7.5-mV shift of the *I-V* curve in January et al. (1988). The activation time constant τ_d at all potentials is reduced by 11%. A 10-mV shift in the negative direction of the steady state inactivation curve, f_∞, of I_{Ca} is introduced. A similar shift is applied to the time constant curve τ_f of this process. In addition, its values at all potentials are reduced by 5% to reflect the acceleration of inactivation of I_{Ca} in the presence of Bay K 8644. The *I-V* curve of the L-type channel current was computed before and after the simulated effects of Bay K 8644. Simulated behavior is consistent with the experimental observations (January et al., 1988).

Isoproterenol

Isoproterenol is a β-adrenergic agonist. It is known to increase heart rate and to enhance contraction (Gadsby, 1984). By binding to the β-adrenoceptors to activate a particular type of G protein, the agonist can exert multiple effects on cardiac cells. These include enhancement of calcium and potassium channel currents, increased calcium uptake ability of the SR, and modulation of the sodium current and the Na/K pump. Isoproterenol effects on individual processes are described below.

L-type calcium channel

β-adrenergic agents such as isoproterenol enhance the L-type calcium channel current but have no effect on the T-type calcium channel current (Tytgat et al., 1988; Bean, 1985). The enhancement of I_{Ca} depends on the isoproterenol concentration (Trautwein et al., 1987). The threshold, half-maximal, and maximal isoproterenol concentrations are 0.02, 0.2, and 1.0 μM, respectively.

Studies on single channels (Bean et al., 1984; Ochi and Kawashima, 1990; Tsien et al., 1986) have shown that the unitary current amplitude of a single channel remained unchanged with the addition of β-adrenergic agents. Channel openings were prolonged and channel closing was abbreviated. The number of functional channels increased severalfold in the presence of a β-adrenergic agent. This increase was species dependent, bringing about an enhancement of the L-type current in the range of 1.5 to 8 fold in whole cell recordings.

To simulate the effects of isoproterenol on the calcium current in a Hodgkin-Huxley type formalism, many investigators suggested simple scaling of the magnitude of I_{Ca}. This adjustment is adequate when guinea pig myocytes are considered. However, a negative shift along the voltage axis of the L-type *I-V* curve and a shift of voltage-dependent activation and inactivation were observed in other species such as frog, rabbit, and rat cardiac cells (Rosen et al., 1990; Bean, 1984; Tiaho et al., 1991). In addition, deceleration of inactivation was also found (Tiaho et al., 1991).

Studies of EADs induced by isoproterenol were performed in isolated canine ventricular cells by Priori and Corr (1990). Detailed published studies of the effects of β-adrenergic agents on canine ventricular myocytes could not be found. In our simulations of the effects of isoproterenol on dog ventricular cells (the choice of a canine cell is dictated by the Priori and Corr study that we are trying to simulate), we do not introduce shifts of the voltage-dependent activation and inactivation curves. The inactivation time constant is increased by 13%. A fivefold increase of the maximal conductance is adopted, on the basis of observations of Tseng et al. (1987) in canine ventricular cells.

As to the modulation of Ca^{2+}-dependent inactivation of the L-type current by β-adrenergic agents, uncertainties still remain. It is well accepted that both voltage- and Ca^{2+}-dependent inactivation exist in cardiac myocytes. Recent studies with gating current by Hadley and Lederer (1991a, b) suggested that Ca^{2+}- and voltage-dependent processes inactivate the L-type channels through independent mechanisms. However, the mechanism underlying the Ca^{2+}-dependent inactivation is still not completely understood (Standon and Stanfield, 1982; Armstrong and Eckert, 1987; Nunoki et al., 1989; Trautwein et al., 1987; Ono and Trautwein, 1991; Kameyama et al., 1986). Independent of the mechanism, isoproterenol clearly reduces Ca^{2+}-dependent inactivation. To simulate Ca^{2+}-dependent inactivation in the presence of 1 μM isoproterenol in cardiac cells, the half-point concentration for the Ca^{2+}-dependent inactivation (f_{Ca}) formulation in the L-R model is increased from 0.7 to 0.9 μM. In addition, we set a non-zero minimum value of 0.03 for f_{Ca} to insure that even a very large value of $[Ca^{2+}]_i$ does not fully close the L-type channels in the presence of isoproterenol. This modulation is based on the observation by Hadley and Lederer (1991a) that Ca^{2+} current was still prominent when intracellular Ca^{2+} rose so high as to cause irreversible contraction of the cell. The formulation of f_{Ca} after the modulation by isoproterenol is expressed as follows:

$$f_{Ca} = 0.03 + 0.97/(1 + ([Ca^{2+}]_i/0.9 \times 10^{-3})^3) \quad (2)$$

Delayed rectifier potassium channel

The delayed rectifier potassium current, I_K, can be enhanced by a β-adrenergic agonist [60,68], but the inward rectifier potassium current, I_{K1}, is not (Godsby, 1984). Temperature dependence of β-adrenergic modulation

of the potassium current was observed (Walsh et al., 1988, 1989). Over the range of 20–37°C, the isoproterenol-mediated increase of I_K was very temperature dependent with a 2.5-fold increase at 37°C. In the presence of isoproterenol, a 7–15 mV shift in the hyperpolarization direction of the half-maximal potential of the I_K activation curve was observed (Giles et al., 1989; Duchatell-Gourdov et al., 1989). The time constant of the decay of I_K at repolarization after depolarization increased 10%. Decrease of the activation time constant and increase of the deactivation time constant were also observed by Giles et al. (1989).

In the L-R model, the conductance of I_K is regulated by two gates, a voltage-dependent inactivation gate x_i and a voltage- and time-dependent activation gate, x. To simulate the effects of 1 μM isoproterenol at 35–37°C, we shift the activation curve 8 mV in the hyperpolarization direction and also increase the maximal conductance by a factor of 2. The time constant for activation is also shifted 8 mV in the negative direction to reflect a 1.1-fold increase in deactivation time relative to control at −30 mV.

Calcium uptake by the SR

In the presence of a β-adrenergic agonist, faster relaxation after stronger contraction was observed [3]. As it is mostly Ca^{2+} uptake by the SR that lowers $[Ca^{2+}]_i$ in the myoplasm, this observation suggests an enhanced Ca^{2+} uptake ability by the SR. This hypothesis was supported by the observations of LePench and Demaille (1989) and Gasser et al. (1988). Using isolated rat ventricular cell preparations, in the presence of 1 μM isoproterenol, Kurikara and Konishi (1987) observed a threefold increase of peak calcium transient and a 30–40% increase in the rate of calcium decay. Okazaki et al. (1990) observed similar effects. They also observed that a shorter time was needed to reach the peak calcium transient. In our simulation, we increase by 41% the maximal uptake rate ($\bar{I}_{up}$) of Ca^{2+} by the network sarcoplasmic reticulum (NSR) to simulate these effects of isoproterenol.

Na/K pump

The Na/K pump current is influenced by extracellular and intracellular Na^+, K^+, and Ca^{2+} and also by the membrane potential (Rosen et al., 1990). The effects of isoproterenol on the pump are controversial (Rosen et al., 1990; Desilets et al., 1986). Recent studies by Gao et al. (1992) documented calcium concentration-dependent modulation of the pump current by isoproterenol. For $[Ca^{2+}]_i$ >0.1 μM, I_{NaK} increased and saturated at 1.0 μM $[Ca^{2+}]_i$ to a value that was 23% higher than control. For $[Ca^{2+}]_i$ <0.1 μM, I_{NaK} decreased and saturated at 0.01 μM $[Ca^{2+}]_i$ to a value that was 21% smaller than control. In our model, to simplify the simulation, a 20% increase of the maximal pump current ($\bar{I}_{NaK}$) is introduced to reflect the β-adrenoceptor stimulation of the Na/K pump. We do not consider a reduction of I_{NaK} as our simulations involve pacing at fast rates that results in calcium accumulation and a high $[Ca^{2+}]_i$.

Sodium channel

Our simulations of isoproterenol effects on I_{Na} are mostly on the basis of recent studies by Ono et al. (1989). At 1 μM isoproterenol, they observed a 3.4 ± 0.8 mV shift of the inactivation curve of I_{Na} in the hyperpolarization direction. In their studies they assumed that there was only one inactivation process of I_{Na}. It is generally accepted that two (fast and slow) processes control I_{Na} inactivation. In our simulations, we assume that both inactivation gates are shifted by 3.4 mV in the hyperpolarization direction.

RESULTS

EADs, intracellular calcium and calcium release from the SR

It is believed that under conditions of calcium overload, spontaneous calcium release from the SR that activates a transient inward current is the underlying mechanism for the formation of DADs (Cranefield and Aronson, 1988). As both EADs and DADs are membrane depolarizations that are not directly caused by external stimulation, the question arises whether an increase in intracellular Ca^{2+} and spontaneous calcium release from the SR are also involved in the induction of EADs. To address this question, we induce EADs by simulating the effects of cesium on the membrane currents (Fig. 3). EADs induced by cesium were observed experimentally by many researchers (Marban et al., 1986; Bailie et al., 1988; Kadesa and Zipes, 1990). Our simulations follow the experimental protocols of Marban et al. (Marban et al., 1986). In the presence of 10 mM cesium and 2 mM $[Ca^{2+}]_o$, an EAD with an amplitude of 3 mV is observed in the simulations (not shown). The action potential duration is prolonged from 260 ms under control conditions to 900 ms after exposure to cesium. In Fig. 3, the effect of cesium at a concentration between 5 and 10 mM is simulated (the half-maximal potential, $V_{1/2}$, of δ_{Cs} gate is set to −80 mV). In addition, $[Ca^{2+}]_o$ is doubled to 4 mM. An action potential of 830 ms duration with an EAD of 17 mV amplitude is observed (Fig. 3*A*). These results are consistent with the observations of Marban et al. and demonstrate that EADs can

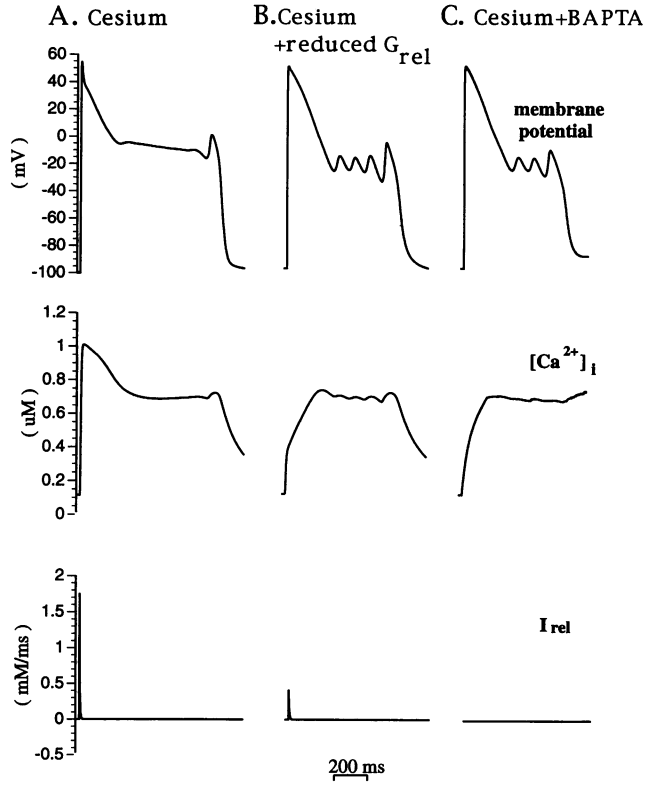

FIGURE 3 From top to bottom, membrane potential, $[Ca]_i$, and I_{rel} are shown. (*A*) In the presence of 4 mM $[Ca^{2+}]_o$, the effect of cesium (between 5 and 10 mM) is simulated by shifting the half-maximal potential of δ_{Cs}-gate to −80 mV. An EAD is generated. (*B*) In the presence of 4 mM $[Ca^{2+}]_o$ and 10 mM cesium, the maximal rate constant of the JSR calcium release current, $\bar{G}_{rel}$, is reduced by 90%. The $[Ca^{2+}]_i$ transient is reduced. EADs are still induced. (*C*) The cell is exposed to 10 mM cesium and 4 mM $[Ca^{2+}]_o$ and is loaded with 1.7 mM BAPTA. I_{rel} is not triggered and $[Ca^{2+}]_i$ is small. EADs still develop.

be induced by cesium at both normal and relatively high $[Ca^{2+}]_o$ in our model.

To lower the intracellular Ca^{2+} transient during the action potential, ryanodine and BAPTA were administered in the experiments of Marban et al. Ryanodine is an alkaloid that inhibits Ca^{2+} release from the SR by depleting the calcium storage in the SR at low concentrations. In the simulations, we represent the reduction of SR Ca^{2+} release as a 90% reduction of the maximal rate constant of the JSR Ca^{2+} release current, $\bar{G}_{rel}$. (Note that we do not simulate the process of calcium depletion but only its outcome in terms of reduced calcium release.) In the presence of 10 mM cesium, 4 mM $[Ca^{2+}]_o$, and $\bar{G}_{rel}$ reduced by 90%, four oscillations (EADs) of the membrane potential are observed during the repolarization phase (Fig. 3*B*). Compared with the behavior without any interventions that alter SR release (Fig. 3*A*), the SR calcium release current, I_{rel}, is a substantially smaller as a result of the reduced $\bar{G}_{rel}$ (Fig. 3*B*). The calcium transient that is generated under the condition of reduced $\bar{G}_{rel}$ is also smaller (Fig. 3*B*) and results mostly from Ca^{2+} entry through the L-type channels. However, EADs are still present.

A different method of reducing the intracellular free calcium concentration is by loading the cell with BAPTA. BAPTA is a Ca^{2+} chelator that increases the Ca^{2+}-buffering capacity of the cell. In the simulations, we introduce BAPTA as a third myoplasmic buffer in addition to troponin and calmodulin. Its buffering action is represented by the following equation:

$$[\text{BAPTA}] = \overline{[\text{BAPTA}]} \times \left\{ \frac{[Ca^{2+}]_i}{[Ca^{2+}]_i + K_{m,\text{BAPTA}}} \right\} \quad (3)$$

where [BAPTA] is the concentration of BAPTA that binds calcium, $\overline{[\text{BAPTA}]}$ is the total BAPTA concentration in the myoplasm, and $K_{m,\text{BAPTA}}$ is 0.215 μM based on measurements by Harrison and Bers (1987). In the presence of 1.7 mM BAPTA, 4 mM $[Ca^{2+}]_o$, and 10 mM Cs^+, EADs are present (Fig. 3*C*). No calcium release from the SR is observed as the increase in intracellular free Ca^{2+} is not sufficient to induce SR release. As in the previous simulation (Fig. 3*B*), the $[Ca^{2+}]_i$ increase is also caused by Ca^{2+} entry through the L-type channels. Despite the small $[Ca^{2+}]_i$ transient, EADs are still present.

The simulation results presented in Fig. 3 demonstrate that Ca^{2+} release from the SR is not necessary for EADs to develop and that EADs can be formed in the absence of calcium overload. Therefore, in contrast to DADs, calcium overload and spontaneous release of calcium from the SR are not the basis for the development of EADs.

The role of the L-type calcium current in EAD formation

It is widely accepted that a transient inward current, I_{ti}, at resting potential causes DADs. This current is carried by the Na^+-Ca^{2+} exchanger or, in some cases such as calcium overload, by an additional current through a nonspecific calcium-activated channel (Luo and Rudy, 1994b). In contrast, a controversy still exists as to which current carries the depolarizing charge that causes the secondary depolarization during an action potential, leading to an EAD. To address this question, we simulate the experimental protocols of January et al. (January et al., 1988; January and Riddle, 1989) in which Bay K 8644 was used to induce EADs. With the simulated intervention of 1 μM Bay K 8644, an EAD is induced (Fig. 4*A*). Accompanying the secondary depolarization is a reversal of the direction of change of I_{Ca} that stops decreasing in magnitude and increases in the inward direction, displaying a negative hump during the EAD (Fig. 4*B*, arrow 1). Fig. 4*C* shows that this behavior of I_{Ca} is caused by reactivation of the *d*-gate, which determines the activation kinetics of the L-type calcium channel, from its deactivation state (Fig. 4*C*, arrow 3). The inactivation *f*-gate and f_{Ca}-gate represent the voltage- and calcium-dependent inactivation processes of the calcium channel, respectively. Recovery of both inactivation gates from their inactivation state is observed before the EAD depolarization (Fig. 4*C*). The dynamics of their recovery and their role in EAD development will be discussed in the next section, in conjunction with the conditional phase that precedes the EAD. The Na^+-Ca^{2+} exchange current, I_{NaCa}, reverses its outward-to-inward trend before the EAD take-off and changes from inward to outward during the EAD depolarization phase (Fig. 4*D*, arrow 2). I_K and the total time-independent current, I_V, (Fig. 4, *C* and *D*, respectively) also become more outward at the EAD depolarization phase.

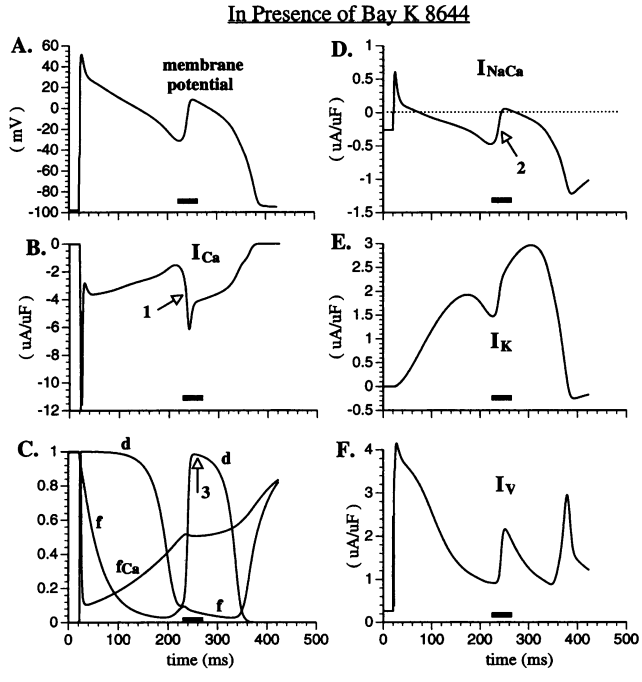

FIGURE 4 EADs in the presence of 1 μM Bay K 8644. (*A*) Action potential with an EAD. (*B*) I_{Ca} during the action potential. (*C*) Kinetic processes of the L-type channel. *d*, activation gate; *f*, voltage-dependent inactivation gate; f_{Ca}, calcium-dependent inactivation gate. (*D*) Sodium-calcium exchange current, I_{NaCa}. (*E*) The delayed rectifier K^+ current, I_K. (*F*) The sum of all time-independent currents, I_v; $I_V = I_{NaK} + I_{K1} + I_{Kp} + I_{Na,b} + I_{Ca,b} + I_{p,Ca}$. Bars in each panel indicate the EAD depolarization phase.

(Note that all time-independent currents are lumped together and represented as I_V; $I_V = I_{NaK} + I_{K1} + I_{Kp} + I_{Na,b} + I_{p,Ca}$). I_{Na} (not shown) remains zero just before, during, and after the EAD. Therefore in the simulations of EADs induced by Bay K 8644, I_{Ca} is the only current that increases in the inward direction during the EAD depolarization phase and develops a larger inward magnitude during the EAD than during normal, uninterrupted repolarization. I_{NaCa}, although mostly inward during the EAD depolarization phase, is of small magnitude. In fact, following its voltage-dependence characteristics, it becomes less inward as a result of the EAD depolarization and contributes less depolarizing current than in the absence of the EAD. All of the other currents become more outward during the same period and, in fact, provide more repolarizing currents at the EAD depolarization phase than when an EAD is not generated, counteracting the depolarization process that is supported by I_{Ca}. Similar behavior is also observed in the simulations when EADs are induced by cesium or by isoproterenol.

As stated above, I_{Ca} is the only current that increases in the inward (depolarizing) direction during the EAD depolarization phase and that develops a larger inward magnitude in the presence of an EAD than in its absence. I_{NaCa}, on the other hand, reduces its inward magnitude and becomes outward at the end of the EAD depolarization phase. However, it is still inward during most of this phase. To evaluate the importance of these inward currents to the depolarization process that generates the EAD, we conducted the following simulations. The reactivation and inward increase of I_{Ca} were prevented by clamping its magnitude at a constant value from the time when secondary depolarization began in the absence of an I_{Ca} clamp. As shown in Fig. 5*A*, fast secondary depolarization does not occur when I_{Ca} reactivation is prevented. In contrast, if I_{NaCa} is clamped to zero starting at the same time (Fig. 5*B*) and no clamp is imposed on I_{Ca}, fast secondary depolarization and an EAD develop. We conclude that I_{Ca} is essential as a depolarizing charge carrier for the secondary depolarization and EAD development. In contrast, I_{NaCa} is not necessary for carrying the depolarizing charge for EAD development.

January and Riddle (1989) studied the role played by I_{Ca} in EAD development using a two-step voltage clamp protocol. This protocol is simulated by our computer model as shown in Fig. 6. When the cell is released from the two-step voltage clamp, the membrane depolarizes and a hump similar in morphology to an EAD is produced. This EAD amplitude, measured from the second voltage step (V_{sc}), is larger at more negative V_{sc} ($V_{sc} = -20$ mV and $V_{sc} = -50$ mV are shown in Fig. 6*A*). Fig. 6*D* shows the EAD amplitude as a function of V_{sc} (solid circles). The simulated increase of the EAD magnitude as V_{sc} is held at more negative potentials is consistent with January and Riddle's experimental observation. Our results also show that the EAD amplitude is dominated by I_{Ca} the magnitude of which is much larger than that of I_{NaCa}. In Fig. 6, *B* and *C*, I_{Ca} and I_{NaCa} are compared at two different V_{sc}, −20 and −50 mV. At V_{sc} of −50 mV, I_{Ca} has a magnitude that is about six times larger than at V_{sc} of −20 mV (Fig. 6*B*). The larger I_{Ca} is associated with an EAD amplitude that is approximately four times larger (Fig. 6*A*). In contrast, I_{NaCa} is more outward at −50 mV (Fig. 6*C*), counteracting the increase in the EAD amplitude. In Fig. 6*D*, we show the EAD amplitude and peak I_{Ca} magnitude as a function of V_{sc}. Both have a similar dependence on V_{sc}, which also suggests that the increase in I_{Ca} is responsible for the larger EAD amplitude at more negative V_{sc}.

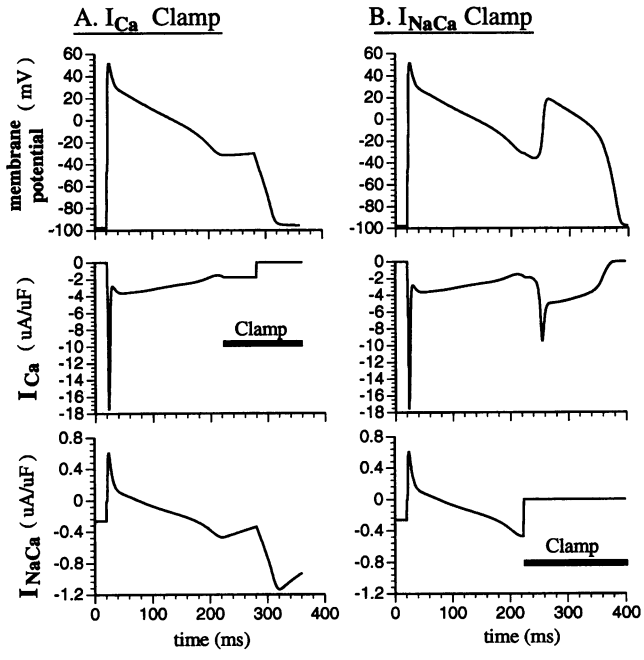

FIGURE 5 (*A*) In the presence of 1 μM Bay K 8644, reactivation of I_{Ca} is prevented by clamping it at a constant value from the time when secondary depolarization begins in the absence of the I_{Ca} clamp. Fast secondary depolarization does not occur (top panel). Corresponding I_{Ca} and I_{NaCa} are shown in the middle and bottom panels. (*B*) In the presence of Bay K 8644, I_{NaCa} is clamped to zero from the same time as above. I_{Ca} is not clamped. An EAD still develops. Corresponding I_{Ca} and I_{NaCa} are shown in the middle and bottom panels.

In conclusion, our simulations demonstrate that secondary reactivation during the plateau of the L-type calcium current is necessary for EAD formation. During the EAD depolarization phase, I_{Ca} is essential as a depolarizing charge carrier and a larger I_{Ca} is associated with a larger EAD. I_{NaCa} is not necessary for EAD depolarization. Other currents become more outward during the EAD, countering secondary depolarization and EAD development.

Effects of calcium and potassium currents during the EAD conditional phase

A delay of repolarization during the plateau of the action potential is generally observed when an EAD develops. January et al. introduced the concept of an EAD conditional phase defined as the repolarization phase before the EAD occurs. During this phase, the total transmembrane ionic current (I_{total}) is small and outward. I_{Ca} and I_K are two major time-dependent currents present during this phase, before the

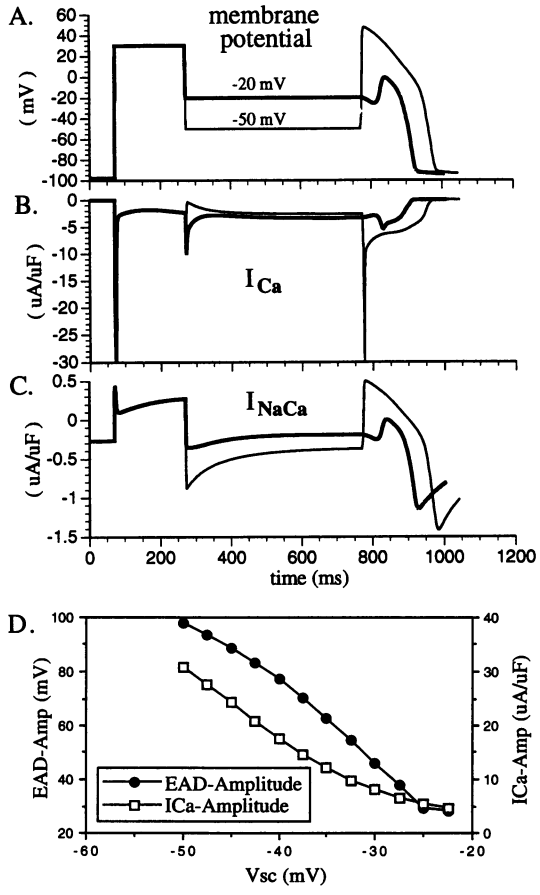

FIGURE 6 Two-step voltage-clamp protocols are simulated. The membrane is first clamped to 20 mV for 200 ms and then to different plateau potentials (V_{sc}) for 500 ms. (*A*) Membrane potentials at V_{sc} of −20 (bold) and −50 (thin) mV are compared. After the release of the clamp, a hump similar in morphology to an EAD is developed. EAD amplitude, measured from V_{sc}, is larger at V_{sc} of −50 mV. (*B*) Corresponding I_{Ca}. (*C*) Corresponding I_{NaCa} at V_{sc} of −20 (bold) and −50 (thin) mV. (*D*) Peak I_{Ca} (open squares) and EAD amplitude (solid circles) are shown as a function of V_{sc}.

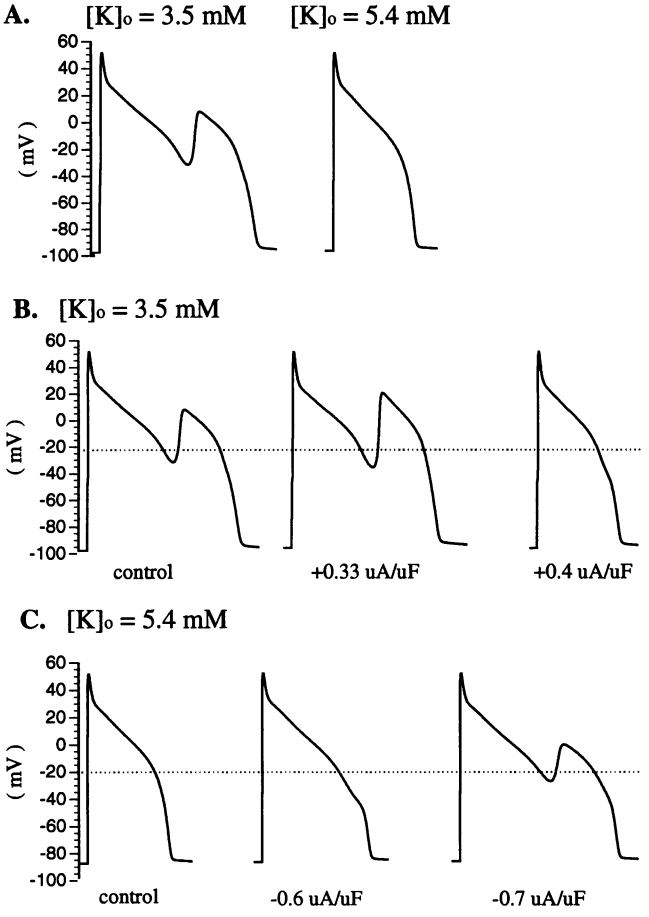

FIGURE 7 (*A*) In the presence of 1 μM Bay K 8644, EAD is induced at 3.5 mM $[K^+]_o$ (left) but not at 5.4 mM $[K^+]_o$ (right). (*B*) At 3.5 mM $[K^+]_o$, constant outward currents of different magnitudes as marked under the figure are applied to the cell. EADs are abolished with a sufficiently large outward current (right column, 0.4 μA/μF). (*C*) At 5.4 mM $[K^+]_o$, constant inward currents of different magnitudes as marked under the figure are applied. EADs are induced with a sufficiently large inward current (right column, −0.7 μA/μF).

EAD take-off. Using the L-R model, we investigated the behavior of these two currents during the EAD conditional phase.

I_{Ca} is an inward current whereas I_K is a repolarizing (outward) current. The magnitudes of both currents increase and then decrease during the repolarization phase of a normal action potential. In the previous sections, we have demonstrated that cesium can induce EADs by reducing the outward K^+ current and Bay K 8644 can induce EADs by enhancing the inward Ca^{2+} current. Either intervention results in a net transmembrane inward current and creates conditions that are favorable for an EAD to develop. In contrast, EADs can be removed by reducing inward currents or enhancing outward currents. The simulations in Fig. 7 demonstrate that application of Bay K 8644 to an extracellular solution that contains 3.5 mM K^+ induces an EAD in the cell model (Fig. 7*A*, left panel). If $[K^+]_o$ is increased from 3.5 to 5.4 mM, the EAD is removed (Fig. 7*A*, right panel). I_K and I_{K1} are known to be $[K^+]_o$ dependent, a property that is simulated in our model. At high $[K^+]_o$, the conductances of these two channels increase, resulting in an increase of these outward currents and acceleration of repolarization. Even when $[K^+]_o$ is maintained at 3.5 mM, the EAD can be removed by applying a constant outward current of sufficient magnitude (>0.4 μA/μF; Fig. 7*B*). EAD is not induced by Bay K 8644 at 5.4 mM $[K^+]_o$. However, if a constant inward current is applied to the cell (Fig. 7*C*), the duration of the action potential increases with the magnitude of this current and EAD is induced when this current is sufficiently large (>0.7 μA/μF). The above simulation results are consistent with the experimental observations of January et al. [30]. It is important to note that the applied current used to induce or remove EADs is less than 0.7 μA/μF in magnitude. This value is quite small compared with I_{Ca} and I_K (range, from 3 to 8 μA/μF) but falls within the range of I_{NaCa}. The results demonstrate that small changes in I_{total} during the conditional phase can affect the formation or removal of EADs.

By exposing the ventricular cell to cesium, EADs are induced (Fig. 8*A*) as was demonstrated before (see Fig. 3). If

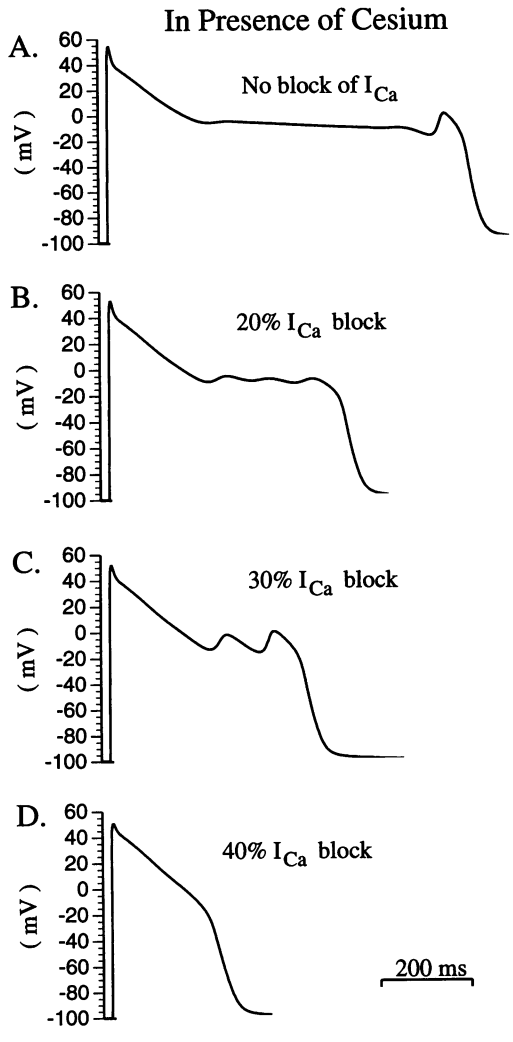

FIGURE 8 The effects of reduction of I_{Ca} on EAD formation. EADs are induced by the simulated effects of cesium as shown in Fig. 3A. The maximal conductance of I_{Ca} is reduced by different percentages as indicated in the figure. EAD is removed when a 40% block is applied.

the maximal conductance of I_{Ca} is reduced to different degrees (from 80 to 60% of its maximal value), the duration of the action potential decreases gradually with increasing blockade of I_{Ca} (Fig. 8, *B-D*) and the EAD disappears when the I_{Ca} conductance is reduced to 60% of its maximal value. We conclude that reduction of I_{Ca} accelerates repolarization during the conditional phase and creates conditions that do not favor EAD formation. However, once EADs are induced, the basic behavior of I_{Ca} and other currents and their contribution to EADs are the same as shown in Fig. 4.

The slowing and delay of repolarization during the EAD conditional phase were observed in the above two simulations. A related question is how prolongation of the plateau enhances EAD formation. To address this question, we examine kinetic processes of the L-type channel (*d*-gate, *f*-gate, and f_{Ca}-gate) when EAD is induced by Bay K 8644 (Fig. 4*C*; I_{Ca} is shown in Fig. 4*B*). After the initial inactivation caused by depolarization and $[Ca^{2+}]_i$ increase, both inactivation gates, *f*-gate and f_{Ca}-gate, gradually recover at a relatively slow rate with repolarization. This process is also observed during normal repolarization without an EAD (demonstrated by the L-R model (Luo and Rudy, 1994a)). Unlike the inactivation gates, the activation d-gate of the L-type channel has a very fast time constant. To a good approximation, its time dependence can be neglected during the repolarization phase of the action potential. Hence the value of *d* is basically determined by the membrane potential. After its fast initial activation at the beginning of the action potential, the *d*-gate deactivates with repolarization. At the EAD take-off potential range, the *d*-gate is not fully deactivated. With the delay of repolarization, *f* and f_{Ca} are allowed longer recovery time and attain a state of greater reactivation. Therefore, when the membrane repolarizes to the same potential level at a slower rate, the conductance of the L-type I_{Ca} at this potential is larger than that during repolarization at a normal rate. Hence, with delayed repolarization, more inward current is produced by I_{Ca} at the conditional phase, leading to conditions that favor EAD formation.

The important conclusions regarding the effects of I_{Ca} and I_K during the conditional phase for EAD formation can be summarized as follows: 1) increase of I_{Ca} or decrease of I_K during the conditional phase helps conditions for EAD to develop; 2) a small change in total transmembrane ionic current during the conditional phase is sufficient to influence EAD formation; and 3) slowing and delay of repolarization during the conditional phase allow longer time for I_{Ca} to recover from inactivation, which in turn results in a larger inward transmembrane current contributed by I_{Ca}, leading to conditions that favor EAD formation. We observe that small changes in the membrane current during the conditional phase can greatly influence EAD formation. These observations demonstrate the delicate balance between currents that exists during the action potential plateau and the high sensitivity to small changes during this phase.

Role of Na-Ca exchange current during the EAD conditional phase

Two reasons motivate us to investigate the effects of I_{NaCa} on the conditional phase and its role in the development of EADs. The first reason is that the magnitude of the added current needed to induce or remove EADs is small and falls in the range of the I_{NaCa} magnitude. This was demonstrated previously (Fig. 7). The second reason is the hypothesis of Priori and Corr (1990) that EADs share the same mechanism as DADs, namely spontaneous Ca^{2+} release from the SR that activates an inward transient current, possibly I_{NaCa}, to depolarize the membrane. With isoproterenol in the extracellular solution, they observed the appearance of both EADs and DADs when a ventricular cell was paced at a rate of 1–2 Hz. Interventions that abolish DADs, such as block of Ca^{2+} release from the SR and reduction of inward I_{NaCa} (a candidate for I_{ti}) also caused EADs to disappear in their experiments. Their conclusion is in disagreement with our simulations presented so far that used cesium or Bay K 8644 to induce EADs. Our studies identify that reactivation of I_{Ca} is

the mechanism of EAD formation, different from the activation of I_{NaCa} that results in DADs.

To study whether I_{NaCa} plays a role in the production of EADs, isoproterenol, used experimentally by Priori and Corr, is also used in our simulations. The ventricular cell is paced at a drive cycle length (CL) of 600 ms, which is similar to the rate used by Priori and Corr. In the presence of isoproterenol, EADs are induced when the cell is paced at a CL of 600 ms. In the simulation, the cell is stimulated 36 times and EADs begin from the 15th stimulated action potential. After termination of pacing, DADs are observed. Each DAD is accompanied by a calcium release from the JSR and an intracellular calcium transient as shown in Fig. 9 in which the last paced action potential and the first DAD are shown. Fig. 10 depicts the corresponding transmembrane L-type Ca^{2+} current as well as the Na^+-Ca^{2+} exchange current. A second

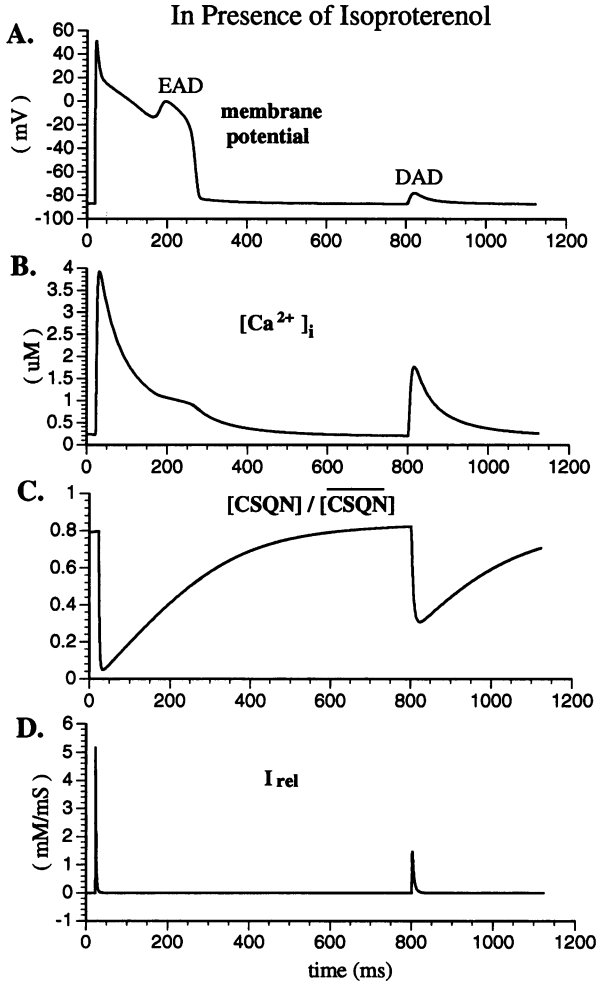

FIGURE 9 In the presence of 1 μM isoproterenol, the ventricular cell model is paced at a CL of 600 ms. (*A*) The last paced action potentials are shown. Membrane potential after termination of pacing is also shown and displays a DAD. (*B*) corresponding $[Ca^{2+}]_i$. (*C*) Corresponding percentage of calsequestrin (CSQN, calcium buffer in JSR) that is occupied by calcium. (*D*) I_{rel}, the release of Ca^{2+} from JSR to the myoplasm. In contrast to DAD, EAD does not involve Ca^{2+} release by the SR (*C* and *D*). The slight increase in $[Ca^{2+}]_i$ during the EAD (*B*) is caused by Ca^{2+} entry through the L-type channels when I_{Ca} is reactivated.

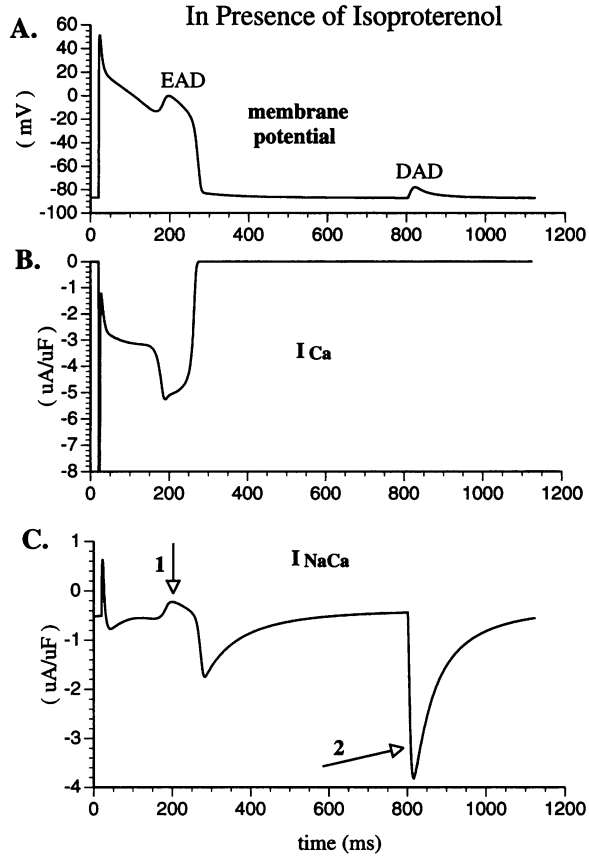

FIGURE 10 (*A*) Last paced action potential and first triggered DAD in Fig. 9*A* are repeated. (*B*) Corresponding I_{Ca}. (*C*) Corresponding I_{NaCa}. I_{Ca} (*B*) is a depolarizing current during the EAD, but not during the DAD; I_{NaCa} (*C*) is a large depolarizing current during the DAD (arrow 2), but small and decreasing during the EAD (arrow 1).

SR calcium release is not observed during the EAD (Fig. 9, *C* and *D*). The slight increase in $[Ca^{2+}]_i$ during the EAD (Fig. 9*B*) is caused by Ca^{2+} entry through the L-type channels when I_{Ca} is reactivated. As was demonstrated before, when cesium and Bay K were used to induce EADs, I_{Ca} is the only current that becomes more inward during the EAD depolarization phase. I_{Na} remains zero. I_{NaCa} and all the other currents change toward a more outward direction in the same period. When EADs are induced by isoproterenol (Fig. 9), the $[Ca^{2+}]_i$ transient has a peak value between 3 and 4 μM during the paced action potential (three to four times its value under normal conditions in the absence of isoproterenol). As a result, I_{NaCa} (Fig. 10*C*) is mostly inward during the EAD conditional phase with an average magnitude between 0.6 and 0.8 μA/μF. During the EAD depolarizing phase, I_{NaCa} remains inward but its magnitude decreases quickly and is much smaller than that of I_{Ca} (arrow 1). In other words, although during the entire repolarization phase of the action potential I_{NaCa} is inward and contributes to the depolarization of the membrane, it is clear that there is less contribution during the EAD depolarizing phase than at other times. In contrast, a very large inward transient of I_{NaCa} is induced by the $[Ca^{2+}]_i$ transient at the DAD depolarizing phase (arrow

2). This result is consistent with the generally accepted mechanism responsible for the occurrence of DADs. Our simulation results clearly suggest that EADs and DADs do not share the same mechanism. Even in the presence of isoproterenol, EADs require reactivation of I_{Ca} whereas DADs require Ca^{2+} release from the SR and activation of the transient inward current.

If I_{NaCa} is not the depolarizing charge carrier during EADs, why do interventions that reduce the inward magnitude of I_{NaCa} abolish EADs (as well as DADs) induced by isoproterenol in the experiments of Priori and Corr? To address this question, we simulate the experimental interventions used by Priori and Corr (1990).

In the presence of isoproterenol, when the cell is paced at a CL of 600 ms, both EADs and DADs develop (Fig. 11*A*). In the simulation of Fig. 11*B*, isoproterenol is present and extracellular Na^+ concentration, $[Na^+]_o$, is reduced from 140 to 40 mM. This intervention reduces the inward driving force on I_{NaCa}. After a 2-min exposure to the above environment without any stimulation, we find that the intracellular Na^+ concentration, $[Na^+]_i$, is decreased from 10 mM and reaches a relatively stable value around 2.6 mM. Then the cell is paced at a CL of 600 ms (Fig. 11*B*). Both EADs and DADs are abolished (cf. Fig. 11, *A* and *B*) although the maximum Ca^{2+} transient during the action potential is larger than that under normal $[Na^+]_o$ and Ca^{2+} is still spontaneously released from the SR after pacing is terminated. The next intervention that affects I_{NaCa} is reduction of the maximal conductance of $\bar{I}_{NaCa}$ by 85% from the time marked by the arrow in Fig. 11*C*. This intervention is similar to the effect of benzamil, an analogue of amiloride known to block Na^+-Ca^{2+} exchange. Both EADs and DADs are abolished despite the large Ca^{2+} transient and the spontaneous release of Ca^{2+} from the JSR that still occurs. The last intervention that acts to reduce I_{NaCa} is reduction of the $[Ca^{2+}]_i$ transient by blocking SR calcium release. The maximal magnitude of the calcium release flux is reduced by 90% starting at the time marked by the arrow in Fig. 11*D*. The $[Ca^+]_i$ transient during the action potential is reduced markedly. Both EADs and DADs disappear.

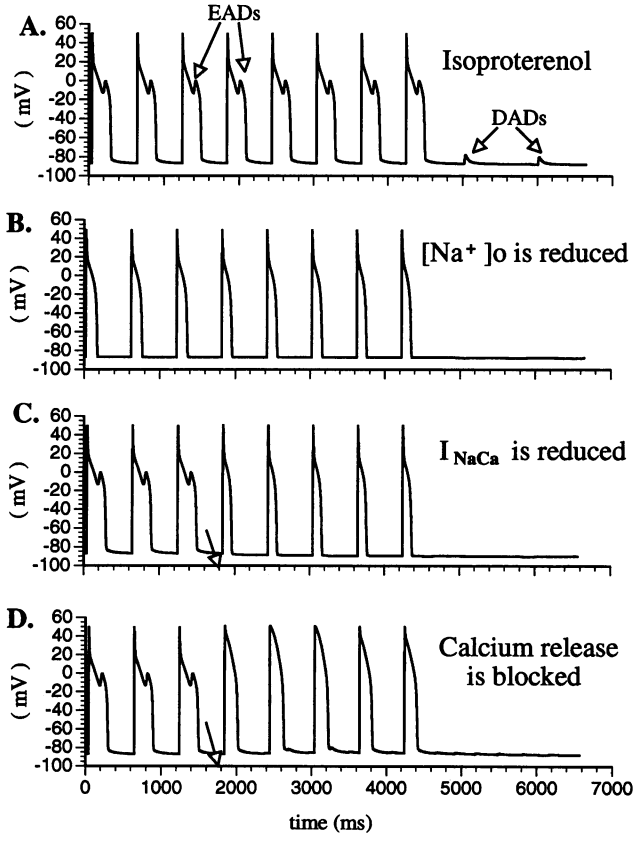

FIGURE 11 In the presence of isoproterenol, the cell is paced at a CL of 600 ms and three different interventions are applied. (*A*) With isoproterenol alone (no other intervention), both EADs and DADs develop. (*B*) $[Na^+]_o$ is reduced from 140 to 40 mM. The cell is kept at diastolic potential for 2 min after the change of $[Na^+]_o$ and the cell is then paced 14 times. The last 8 paced action potentials are shown. (*C*) The maximal conductance of I_{NaCa} is reduced by 85% starting from the arrow. (*D*) The maximal conductance of I_{rel}, $\bar{G}_{rel}$, is reduced by 90% starting from the time marked by the arrow. All three interventions in *B*, *C*, and *D* abolish the EADs and DADs induced by isoproterenol.

The above simulation results are consistent with the experimental observations of Priori and Corr. To investigate why interventions that abolish DADs can also remove EADs in this case, additional studies are required. When EADs are present, conditions for an EAD formation are met during the EAD conditional phase, meaning that the total transmembrane current can change from outward to inward during the plateau of the action potential. As we have demonstrated that I_{NaCa} is not the depolarizing charge carrier during the EAD depolarizing phase, inhibition of EADs by reduction of I_{NaCa} should result from the inability to satisfy the conditions for EAD formation during the EAD conditional phase.

With this hypothesis in mind, we try to explain why a block of SR calcium release removes EADs induced by isoproterenol but not EADs induced by cesium. We compare I_{NaCa} during normal and reduced SR calcium release for the preparations with cesium or isoproterenol (Fig. 12). In the presence of normal SR release, I_{NaCa} during the conditional phase has a larger inward magnitude with the application of isoproterenol (~ -0.6 $\mu A/\mu F$) than with the application of cesium (~ -0.1 $\mu A/\mu F$). So its contribution to I_{total} during the conditional phase for EAD development is more important in the presence of isoproterenol than in the presence of cesium. The previous simulations have demonstrated that EADs can be induced if a 0.7 $\mu A/\mu F$ constant inward current is applied to the myocyte (Fig. 7*C*). Hence a 0.6 $\mu A/\mu F$ inward I_{NaCa} is an important current component of I_{total} during the EAD conditional phase. The relatively greater inward I_{NaCa} in the presence of isoproterenol is caused by the large $[Ca^{2+}]_i$ transient during the action potential, which is three to four times that under normal conditions, in the absence of isoproterenol. Under these conditions, when SR calcium release is prevented, there is a large magnitude reduction of the $[Ca^{2+}]_i$ transient and I_{NaCa} becomes mostly outward rather than inward during the plateau phase (Fig. 12*A*). This adds a component of outward current during this phase and changes the balance of currents in a way that is not favorable for EAD formation. In contrast to isoproterenol, cesium

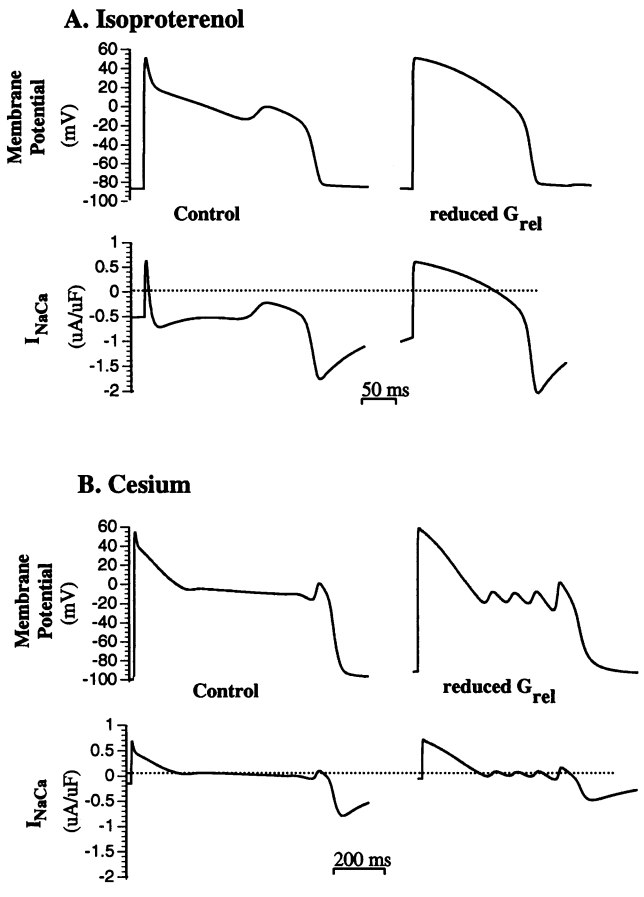

FIGURE 12 The effects of G_{rel} reduction by 90% on membrane potential and I_{NaCa} during EADs induced by isoproterenol or cesium. (*A*) In the presence of isoproterenol. The simulations in Figs. 9*A* and 11*C* are repeated. I_{NaCa} (lower panel) is shown before (left) and after (right) G_{rel} reduction. (*B*) In the presence of Cs^+. The simulations in Fig. 3, *A* and *B* are repeated. I_{NaCa} (lower panel) is shown before (left) and after (right) G_{rel} reduction. Note that the EAD induced by isoproterenol (*A*) is abolished but the EAD induced by cesium (*B*) is not.

blocks only outward K^+ current and does not affect significantly the $[Ca^{2+}]_i$ transient (it is approximately the normal value of 1 μM in Fig. 3, left panel). Therefore, when SR calcium release is prevented in the presence of cesium, the magnitude change of the calcium transient is small, a major shift in the direction of I_{NaCa} is not observed, and I_{total} is minimally affected (Fig. 12*B*). In conclusion, in the presence of isoproterenol, a relatively large inward magnitude of I_{NaCa} during the plateau phase and a large reduction of I_{NaCa} when SR calcium release is prevented is the underlying mechanism for the removal of EADs by reducing SR calcium release. Clearly, at a relatively high $[Ca^{2+}]_i$, I_{NaCa} is more inward during the EAD conditional phase and its contribution can be as important as that of I_K and I_{Ca} for meeting the conditions for EAD formation. Note that although in the presence of a large $[Ca^{2+}]_i$ transient, I_{NaCa} is important for EAD formation because of its effect on the conditional phase, it is still I_{Ca} that carries the depolarizing charge during the EAD.

Lowering $[Na^+]_o$ reduces the inward driving force on the Na^+-Ca^{2+} exchanger and benzamil decreases the conductance of the exchanger. Both interventions remove EADs without significant reduction of the $[Ca^{2+}]_i$ transient (Fig. 13, *B* and *C*). At the plateau phase, the rate of repolarization is very slow, which implies that the total ionic current has a very small outward magnitude. In the presence of isoproterenol, I_{NaCa} (without the interventions of Fig. 13, *B* and *C*) has relatively large inward magnitude. I_{NaCa} under these conditions is a very important current component for supporting the plateau. Once this component is reduced, the plateau duration is shortened. Prominent reduction of the magnitude of this current is observed as a result of the two interventions in Fig. 13, *B* and *C*. Hence, the duration of the plateau phase of the action potential is significantly shortened. Because of this, there is no significant time for I_{Ca} to reactivate and to generate an EAD.

In conclusion, although in some cases I_{NaCa} may remain inward during the EAD depolarizing phase, its magnitude during this phase is much smaller than during the preceding conditional phase. Therefore, I_{NaCa} does not contribute significantly to the EAD depolarization process that is supported by I_{Ca} during the EAD depolarization phase. I_{NaCa} may play a secondary role in EAD formation. It may affect the balance of transmembrane currents during the EAD condi-

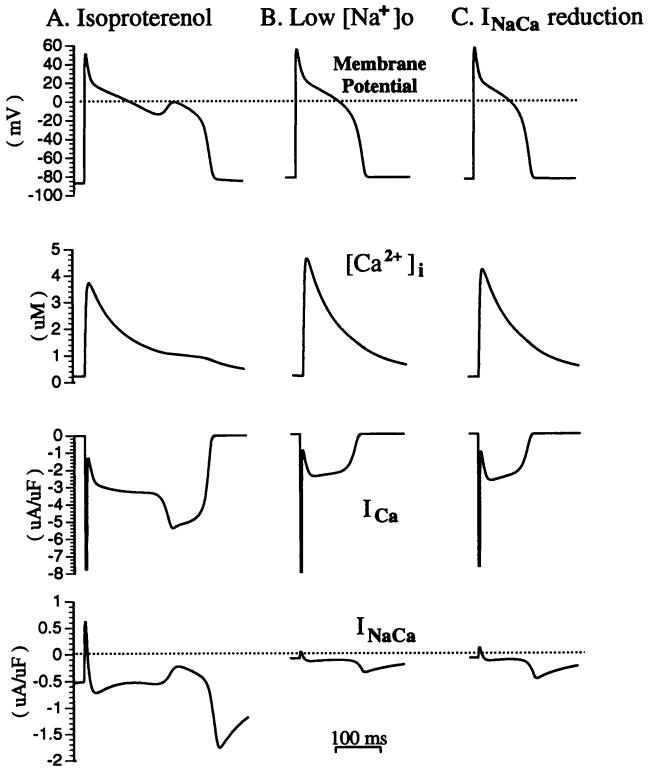

FIGURE 13 From top to bottom, action potential, $[Ca^{2+}]_i$, I_{Ca}, and I_{NaCa} in the presence of isoproterenol with or without interventions that reduce inward I_{NaCa}. The cell is paced at a CL of 600 ms and the behavior during one action potential is shown. (*A*) In the presence of isoproterenol without any other interventions. (*B*) $[Na^+]_o$ is reduced from 140 to 40 mM. (*C*) The effect of reduced I_{NaCa} as in Fig. 11*B* is simulated. The interventions in *B* and *C* reduce I_{NaCa} (bottom panel) and abolish the EAD (top panel). Note that when the EAD is abolished (*B* and *C*), I_{Ca} does not display secondary reactivation during the action potential.

tional phase. This in turn determines whether conditions that favor EAD formation can be developed. At relatively high $[Ca^{2+}]_i$, I_{NaCa} has a relatively large inward magnitude and prolongs the plateau. This allows for sufficient time for reactivation of I_{Ca} and for the generation of EADs.

Rate dependence of EADs

To investigate the rate dependence of EADs, we simulate the following protocols that were conducted experimentally by Damiano and Rosen (1984). A single cell is exposed to a normal Tyrode solution (4 mM K^+) to which 5 mM Cs^+ is added. The cell is paced at different CLs. As shown in Fig. 14, EADs are induced during slow pacing (CL > 1000 ms) whereas at fast pacing rates, EADs are removed. DADs are induced when the cell is paced very fast (CL ≤ 300 ms) causing calcium accumulation and calcium overload conditions (the mechanism of DADs due to calcium overload was investigated in (Luo and Rudy, 1994b)). The behavior in Fig. 14 is consistent with the experimental observations of Damiano and Rosen (1984).

To elucidate the mechanism underlying the rate dependence of EADs, we compare the behavior of the L-type calcium current, I_{Ca}, and the delayed rectifier potassium current, I_K, at CLs of 600 and 1200 ms (Fig. 15). These currents are important determinants of the membrane behavior during the plateau phase and the early repolarization phase. As the major contributors to the total transmembrane current, they influence significantly the balance of currents during the conditional phase. At the slower rate (CL = 1200 ms), the relative contribution of I_{Ca} (inward, depolarizing) and of I_K (outward, repolarizing) is such that the total membrane current becomes inward, and conditions for EAD development are met. As can be seen in Fig. 15*B*, I_{Ca} obtains a larger magnitude at the faster rate. On the basis of previous simulations, this behavior should favor the appearance of EADs at this rate. As EADs actually disappear, other currents must neutralize the depolarizing effects of I_{Ca}. Comparing I_K at the two CLs (Fig. 15*C*), we observe that this current increases faster during the early plateau phase at the faster pacing rate

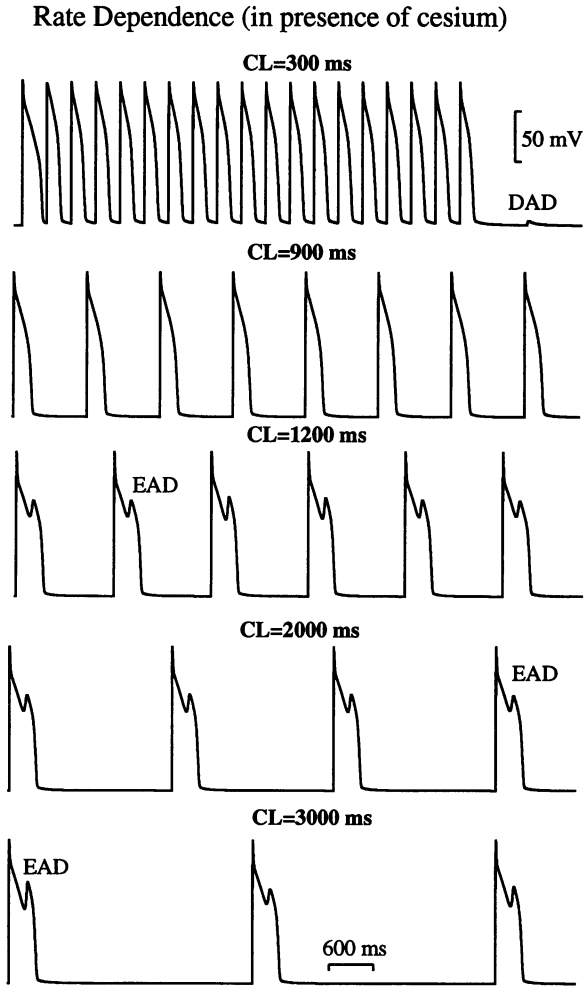

FIGURE 14 EADs induced by cesium at different pacing rates. The cardiac ventricular cell is exposed to Tyrode solution with 4 mM K^+ and 5 mM cesium. It is stimulated periodically at different CLs as marked in the figure. EADs are induced at CL > 1000 ms. ADAD is generated when the cell is paced very fast (CL ≤ 300 ms).

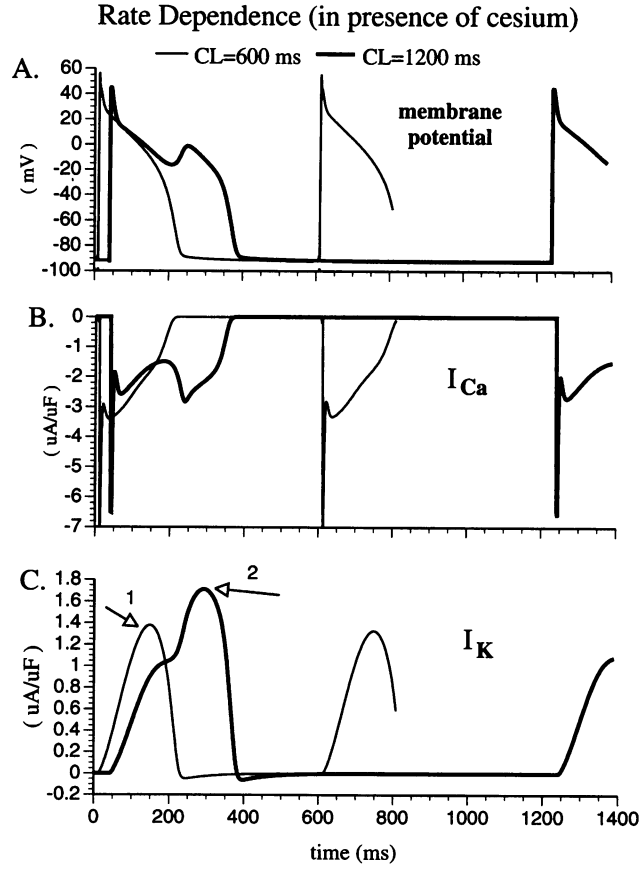

FIGURE 15 I_{Ca} and I_K at two different pacing rates. The simulation described in Fig. 14 is repeated. The action potential, I_{Ca}, and I_K at two different CLs, 600 and 1200 ms, are compared in *A*, *B*, and *C*. I_{Ca} has a larger magnitude at the faster rate. I_K also has a larger magnitude at the fast rate (arrow 1). (The increase of I_K caused by the EAD that is generated at the slower rate (arrow 2) should not be considered in the comparison.)

(Fig. 15*C*, CL = 600 ms, arrow 1). Note that the late large maximum of I_K at the slow pacing rate (Fig. 15*C*, arrow 2) should not be considered in the comparison as it is caused by the voltage dependence of I_K during the EAD rather than being a factor in the EAD formation. The increase of I_K counteracts the increase of I_{Ca} at the faster pacing rate. The relative contribution of the two currents is such that the total current during the conditional phase becomes outward, conditions for EAD development are not met, and the EAD is removed.

To explain the larger magnitude of I_{Ca} and I_K at the faster pacing rate, the underlying kinetic processes are further elucidated in Figs. 16 and 17. At the faster rate, because less Ca^{2+} is extruded from the cell by the Na^+-Ca^{2+} exchanger during the diastolic period, the intracellular Ca^{2+} concentration (Fig. 16*A*) is relatively higher just before each pacing stimulus (arrow) is applied (at CL = 600 ms, $[Ca^{2+}]_i$ = 0.18 μM; at CL = 1200 ms, $[Ca^{2+}]_i$ = 0.14 μM). This causes a higher degree of Ca^{2+}-dependent inactivation of the L-type

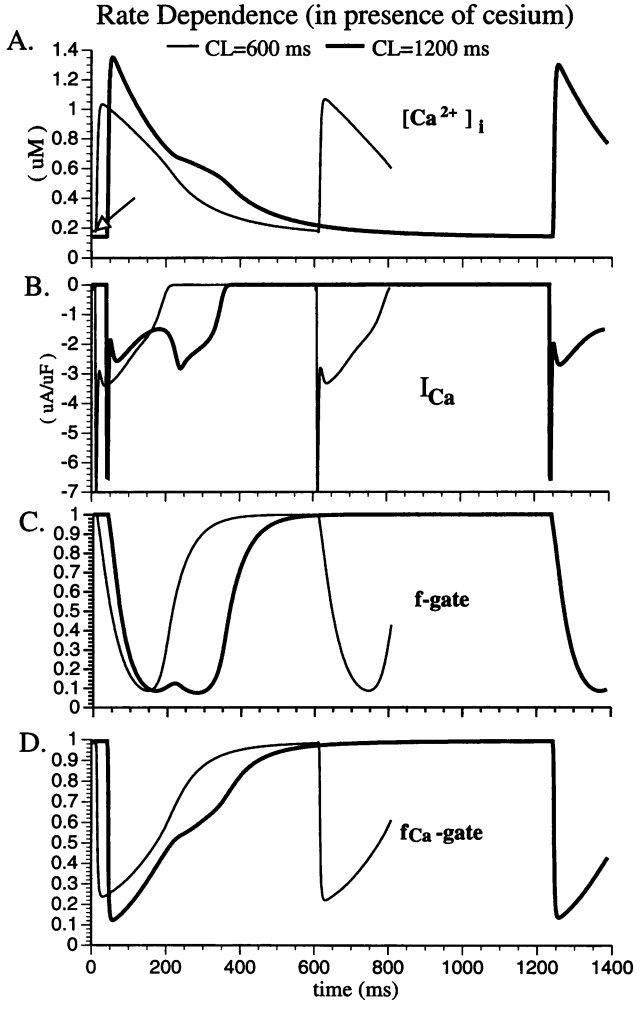

FIGURE 16 The effect of pacing rate on I_{Ca}. In the presence of cesium, $[Ca^{2+}]_i$, I_{Ca}, and its voltage- and calcium-dependent inactivation parameters, f and f_{Ca}, are shown for two pacing rates. At the faster rate, the $[Ca^{2+}]_i$ transient is smaller. Hence there is less Ca^{2+}-dependent inactivation (f_{Ca} is larger), which results in a larger magnitude of I_{Ca}.

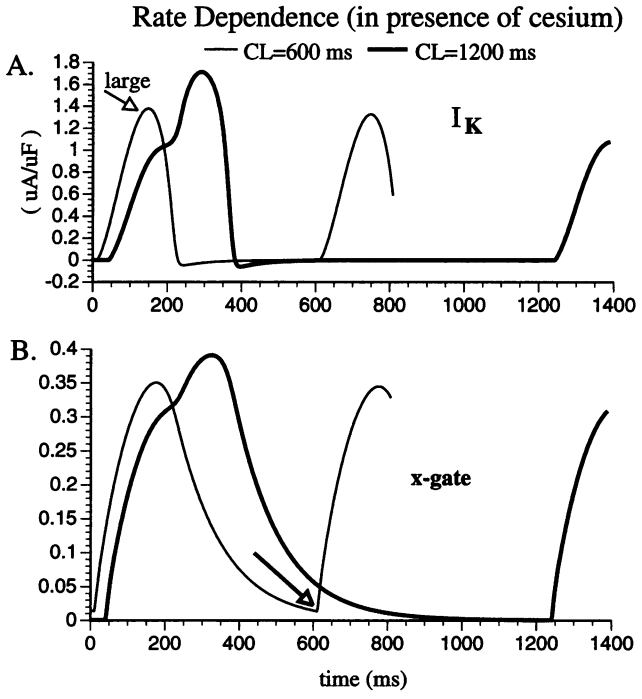

FIGURE 17 The effect of pacing rate on I_K. In the presence of cesium, I_K and its activation parameter are shown for two pacing rates. Immediately before the pacing stimulus, the x-gate is fully deactivated at CL = 1200 ms. However, when CL is only 600 ms, the x-gate is not fully deactivated before each stimulus is applied (arrow in *B*).

channel (see Luo and Rudy, 1994a) and a smaller average I_{Ca} during the first 2 ms of the action potential (Fig. 16*D*), resulting in less Ca^{2+} entry and a smaller Ca^{2+} transient during the plateau phase of the action potential (Fig. 16*A*). This, in turn, results in less Ca^{2+}-dependent inactivation (Fig. 16*D*) and a larger magnitude of I_{Ca} during this phase (Fig. 16*B*). The increase of I_K at the faster pacing rate is related to the large time constant of its activation x-gate (between 130 and 450 ms) (Luo and Rudy, 1994a). After its activation during the action potential, the x-gate requires a long time (~500 ms) to fully deactivate after repolarization. When the cell is paced at a sufficiently fast rate, the pacing stimuli fall at a time when I_K is not completely deactivated (Fig. 17*B*). Beginning from this partially activated state, the conductance of I_K attains a larger value during the action potentials at faster pacing rates as compared with slow pacing rates that permit complete deactivation of the x-gate between paced beats. This results in a larger I_K (Fig. 17*A*) during the plateau phase (the conditional phase) at sufficiently fast pacing rates that, being an outward current, counteracts the depolarizing effect of the enlarged inward I_{Ca} and prevents the formation of an EAD.

DISCUSSION

The theoretical studies presented in this paper are designed to investigate the mechanism of plateau EADs, to help resolve a controversy in the experimental literature regarding

their mechanism, and to help elucidate the mechanism of rate dependence of EADs.

Following published experimental protocols (Marban et al., 1986; January et al., 1988; January and Riddle, 1989; Priori and Corr, 1990), we induced EADs in the ventricular action potential model by simulating the effects of cesium, Bay K 8644, and isoproterenol, respectively. For all of these interventions, the mechanism of EAD depolarization involves secondary reactivation of the L-type calcium channels during the plateau. The reactivated I_{Ca} is essential for EAD development and serves as a depolarizing charge carrier during the EAD depolarization phase. In all cases, prolongation of the action potential plateau is observed when an EAD develops. This, in turn, provides more time at plateau potential for the L-type Ca^{2+} channels to recover from inactivation, a process that involves both the voltage-dependent (f) and calcium-dependent (f_{Ca}) inactivation gates (see Fig. 4). Once sufficient recovery is achieved, I_{Ca} increases its inward magnitude and depolarizes the membrane. This, in turn, causes fast reactivation of the L-type channels through the voltage-dependent characteristics of the activation d-gate (arrow 3 in Fig. 4*C*), resulting in a fast further increase of I_{Ca}. Thus, a positive feedback process that is characteristic of fast depolarization is established by the kinetics of I_{Ca}, leading to EAD formation.

In addition to I_{Ca}, only the Na^+-Ca^{2+} exchange current, I_{NaCa}, is inward during the EAD depolarization phase. However, our simulations suggest that it does not play a primary role in EAD formation. In contrast to the positive feedback kinetics of I_{Ca} at this phase, I_{NaCa} actually decreases quickly upon depolarization. In fact, the inward magnitude of I_{NaCa} is smaller during EAD depolarization than during monotonic repolarization in the absence of an EAD. Thus, the voltage-dependence characteristics of I_{NaCa} and its behavior during the EAD preclude the possibility that it can provide the mechanism for the fast depolarization of the EAD. This conclusion is supported by the fact that fast depolarizing EADs can be generated in the absence of I_{NaCa} during the EAD depolarization phase, but not when reactivation of I_{Ca} is prevented (Fig. 5). It should be mentioned in this context that, in the simulations, the magnitude of I_{NaCa} is much smaller than the magnitude of I_{Ca} during the EAD depolarization phase (Fig. 4). The exact ratio of these magnitudes depends on the relative membrane densities of these ion transfer mechanisms and could be species dependent. However, it is the different kinetics (not the different magnitudes) of I_{Ca} and I_{NaCa} that dictates their very different role during EAD depolarization. An important (but, at this stage, necessary) simplification of our ventricular cell model is the assumption of spatial uniformity inside the cell. In particular, spatial nonuniformity of $[Ca^{2+}]_i$ due to multilocal release sites in the SR, spatial distribution of calcium buffers, restricted spaces, and restricted diffusion is not considered (see Luo and Rudy (1994a, b) for detailed discussion). As a result, the global $[Ca^{2+}]_i$, not the local calcium activity at the exchange site, regulates the Na^+-Ca^{2+} exchange function in the model. Although this approximation does not consider details of the regulation of Na^+-Ca^{2+} exchange on a subcellular scale, I_{NaCa} as formulated in the model simulates correctly its measured voltage dependence and ionic concentration dependence (Luo and Rudy, 1994a). As it is the voltage dependence of I_{NaCa} that causes it to change from inward to outward during the EAD depolarization phase, the conclusion regarding its inability to be the primary depolarizing current for EAD formation should not be affected by the global, cellular level approach. Similar comments apply to the Ca^{2+}-dependent inactivation process of the L-type calcium channels. Inclusion of spatial nonuniformities requires knowledge of the distribution of calcium buffers, of release and uptake sites in the SR, and of the geometry and locations of intracellular organelles. Such detailed geometrical information is not yet available at the present time.

EADs that are induced by cesium are not removed by interventions that reduce the $[Ca^{2+}]_i$ transient and the magnitude of I_{NaCa} (our simulations and experiments of Marban et al. (1986)). In contrast, EADs that are induced by isoproterenol are abolished by interventions that inhibit SR calcium release and reduce I_{NaCa} (our simulations and experiments of Priori and Corr (1990)). The last observation led Priori and Corr to suggest that I_{NaCa} is the primary current responsible for EAD depolarization and that EADs and DADs share the same mechanism (Ca^{2+} release from the SR that triggers *INaCa*). Our simulations demonstrate that a second SR calcium release does not occur during an EAD. The removal of EADs when I_{NaCa} is reduced in the isoproterenol preparation can be explained by the effect of I_{NaCa} on the conditional phase that precedes the EAD. The simulated Priori and Corr protocols generate a large $[Ca^{2+}]_i$ transient (three to four times the normal magnitude of 1.0 μM that is also the magnitude in the cesium protocols). As a result, I_{NaCa} is also large and becomes an important inward component of the total membrane current during the conditional phase. As demonstrated in Results, an EAD can develop if the total transmembrane current becomes inward during the conditional phase. For the isoproterenol protocols, interventions that reduce I_{NaCa} can sufficiently change the balance of currents so that it does not become inward and conditions for EAD formation do not develop. In the case of cesium, I_{NaCa} during the conditional phase is small ($\sim$0.1 μA/μF) and has only a minor effect on the balance of currents. Consequently, interventions that reduce I_{NaCa} do not influence the conditions for EAD development and do not remove the EAD. I_{NaCa} affects EAD generation indirectly, through its effect on the conditional phase that precedes the EAD. The primary mechanism is reactivation of I_{Ca} that depolarizes the membrane to generate the EAD.

Our conclusion that I_{Ca} is the major depolarizing charge carrier during the EAD depolarization phase is based on protocols that involve cesium, Bay K 8644, and isoproterenol. A similar mechanism was also suggested for EADs generated under conditions of calcium overload (Luo and Rudy, 1994b) and by the application of quinidine (Nattel and Quantz, 1988) or cocaine (Kimura et al., 1992). All of these interventions bear a high degree of clinical relevance. However, extreme

modification of the inward fast Na^+ current, I_{Na}, may produce an additional component of inward current during the plateau and induce EADs. Such an intervention was performed by Boutjdir and El-Sherif (1991) and Hiraoka et al. (1992) to study EADs. ATXII (Boutjdir and El-Sherif, 1991) and veratridine (Hiraoka et al., 1992) were used to cause extreme prolongation of I_{Na} inactivation. In fact, the time constant of I_{Na} inactivation is increased ~15-fold by ATXII and ~200-fold by veratridine and becomes similar to or longer than that of I_{Ca} inactivation.

EADs are associated with bradycardia and slow pacing (Cranefield and Aronson, 1988). They may contribute to the polymorphic ventricular arrhythmias in patients with the long QT syndrome that manifest as Torsade de Pointes in the electrocardiogram (Hiraoka et al., 1992; Rosen, 1990). In the simulations, EADs were present at CL > 1000 ms. This behavior is consistent with the experimental observations of Damiano and Rosen (1984) and supports the notion that EADs are bradycardia related. The appearance or disappearance of EADs is determined by the relative contributions of I_{Ca} and I_K to the total membrane current during the conditional phase. At slow rates, the magnitude ratio of I_{Ca} (inward) and I_K (outward) is sufficient to result in an inward total transmembrane current so that conditions for EAD development are met. At fast rates (CL < 1000 ms), the increase in I_K more than offsets the increase in I_{Ca}, resulting in a net outward (repolarizing) current during the conditional phase and in EAD removal.

Several limitations of the model should be mentioned in the context of the EAD study presented here. The model is based mostly on the guinea pig ventricular cell and does not include the transient outward current, I_{to}, which is not present in this cell. In ventricular cells of other species (e.g., dog, rabbit, and rat) I_{to} is a very important current for repolarization and should be included in models of the ventricular action potential and in studies of EADs in these species. Consequently, some of our conclusions may apply only to the guinea pig type of cells and cannot be extrapolated to other types of cells that display a prominent I_{to} or other processes that are not present in the guinea pig myocyte. Another limitation of the model is that the delayed rectifier, I_K, is not separated into its two components, I_{Kr} and I_{Ks}. Therefore, only the role of I_K in its global presentation (as a superposition of I_{Kr} and I_{Ks}) could be investigated. It will be interesting, in future studies, to examine the separate role and relative importance of I_{Kr} and I_{Ks} in repolarization and EAD formation. Work to formulate I_{Kr} and I_{Ks} and to incorporate them in the action potential model is currently conducted in our laboratory.

We wish to thank Dr. Matthew N. Levy and Dr. Robert D. Harvey for helpful discussions.

This study was supported by a National Institutes of Health, National Heart, Lung and Blood Institute Grant HL-49054.

REFERENCES

Armstrong, D., and R. Eckert. 1987. Voltage-activated calcium channels that must be phosphorylated to respond to membrane depolarization. *Proc. Natl. Acad. Sci. USA.* 84:2518–2522.

Bailie, D. S., H. Inoue, S. Kaseda, J. Ben-david, and D. P. Zipes. 1988. Magnesium suppression of early afterdepolarizations and ventricular tachycardias induced by cesium in dogs. *Circulation.* 77:1395–1402.

Bean, B. P. 1984. β-adrenergic regulation of cardiac calcium channels: ionic current and gating current. *Biophys. J.* 57:23*a*. (Abstr.)

Bean, B. P. 1985. Two kinds of calcium channels in canine atrial cells. *J. Gen. Physiol.* 86:1–30.

Bean, B. P., M. C. Nowycky, and R. W. Tsien. 1984. β-adrenergic modulation of calcium channels in frog ventricular heart cells. *Nature.* 307: 371–375.

Boutjdir, M., and N. El-Sherif. 1991. Pharmacological evaluation of early afterdepolarizations induced by sea anemone toxin (ATXII) in dog heart. *Cardiovasc. Res.* 25:815–819.

Cleemann, L., and M. Morad. 1991. Role of Ca^{2+} channel in cardiac excitation-contraction coupling in the rat: evidence from Ca^{2+} transients and contraction. *J. Physiol.* 432:283–312.

Cranefield, P. F., and R. S. Aronson. 1988. Cardiac arrhythmias: the role of triggered activity and other mechanisms. Futura Publishing Company, Inc., New York.

Damiano, B. P., and M. R. Rosen. 1984. Effects of pacing on triggered activity induced by early afterdepolarization. *Lab. Invest.* 69:1013–1025.

Desilets, M., and C. M. Baumgarten. 1986. Isoproterenol directly stimulates the Na^+-K^+ pump in isolated cardiac myoctes. *Am. J. Physiol.* 251:H218–H225.

Duchatelle-Gourdon, I., H. C. Hartzell, and A. A. Largutta. 1989. Modulation of the delayed rectifier potassium current in frog cardiac myocytes by β-adrenergic agonists and magnesium. *J. Physiol.* 415:251–274.

Fabiato, A. 1983. Calcium-induced release of calcium from the cardiac sarcoplasmic reticulum. *Am. J. Physiol.* 245:C1–C14.

Fabiato, A. 1985. Time and calcium dependence of activation and inactivation of calcium-induced release of calcium from the sarcoplasmic reticulum of a skinned canine cardiac Purkinje cell. *J. Gen. Physiol.* 85: 247–289.

Frankowiak, G., M. Bechem, M. Schramm, and G. Thomas. 1985. The optical isomers of the 1,4-Dihydropyridine Bay K8644 show opposite effects on Ca channels. *Eur. J. Pharmacol.* 114:223–226.

Gadsby, D. C. 1984. Beta-adrenoceptor agonists increase membrane K^+ conductance in cardiac Purkinje fibers. *Nature.* 306:691–693.

Gao, J., R. T. Mathias, I. S. Cohen, and G. J. Baldo. 1992. Isoprenaline, Ca^{2+} and the Na^+-K^+ pump in guinea-pig ventricular myocytes. *J. Physiol.* 449:689–704.

Gasser, J., P. Paganetti, E. Carafoli, and M. Chiesi. 1988. Heterogeneous distribution of calmodulin- and cAMP-dependent regulation of Ca^{2+} uptake in cardiac sarcoplasmic reticulum subtractions. *Eur. J. Biochem.* 176:535–541.

Giles, W., T. Nakajima, K. Ono, and E. F. Shibata. 1989. Modulation of the delayed rectifier K^+ current by isoprenaline in bull-frog atrial myocytes. *J. Physiol.* 415:233–249.

Grouselle, M., B. Stuyvers, S. Bonoron-Adele, P. Besse, and D. Georgescauld. 1991. Digital-imaging microscopy analysis of calcium release from sarcoplasmic reticulum in single rat cardiac myocytes. *Pflügers Arch.* 418:109–119.

Hadley, R. W., and W. J. Lederer. 1991a. Ca^{2+} and voltage inactivate Ca^{2+} channels in guinea-pig ventricular myocytes through independent mechanisms. *J. Physiol.* 444:257–268.

Hadley, R. W., and W. J. Lederer. 1991b. Properties of L-type calcium channel gating current in isolated guinea pig ventricular myocytes. *J. Gen. Physiol.* 98:265–285.

Hadley, R. W., and W. J. Lederer. 1992. Comparison of the effects of Bay K 8644 on cardiac Ca^{2+} current and Ca^{2+} channel gating current. *Am. J. Physiol.* 262:H472–H477.

Harrison, S. M., and D. M. Bers. 1987. The effect of temperature and ionic strength on the apparent Ca-affinity of EGTA and the analogous Ca-chelators BAPTA and dibromo-BAPTA. *Biochim. Biophys. Acta.* 925: 133–143.

Harvey, R. D., and R. E. Ten Eick. 1989. Voltage-dependent block of cardiac inward-rectifying potassium current by monovalent cations. *J. Gen. Physiol.* 94:349–361.

Hess, P., J. B. Lansman, and R. W. Tsien. 1984. Different modes of Ca^{2+} channel gating behavior favored by dihydropyridine agonists and antagonists. *Nature.* 311:538–544.

Hirano, Y., A. Moscucci, and C. T. January. 1992. Direct measurement of L-type Ca^{2+} window current in heart cells. *Circ. Res.* 70:445–455.

Hiraoka, M., A. Sunami, F. Zheng, and T. Sawanobori. 1992. Multiple ionic mechanisms of early afterdepolarizations in isolated ventricular myocytes from guinea-pig hearts. *In* QT Prolongation and Ventricular Arrhythmias. K. Hashiba, A. T. Moss, and P. J. Schwartz, editors. The New York Academy of Sciences, New York. 33–34.

Isenberg, G. 1976. Cardiac Purkinje fibers: Cesium as a tool to block inward rectifying potassium currents. *Pflügers Arch.* 365:99–106.

January, C. T., V. Chau, and J. C. Makielski. 1991. Triggered activity in the heart: cellular mechanisms of early afterdepolarizations. *Eur. Heart J.* 12(Suppl F):4–9.

January, C. T., and A. Moscucci. 1992. Cellular mechanism of early afterdepolarizations. *In* QT Prolongation and Ventricular Arrhythmias. K. Hashiba, A. T. Moss, and P. J. Schwartz, editors. New York Academy of Science, New York. 23–32.

January, C. T., and J. M. Riddle. 1989. Early afterdepolarizations: Mechanism of induction and block: a role for L-type Ca^{2+} current. *Circ. Res.* 64:977–989.

January, C. T., J. M. Riddle, and J. J. Salata. 1988. A model for early afterdepolarizations: induction with the Ca^{2+} channel agonist Bay K 8644. *Circ. Res.* 62:563–571.

Kadesa, S., and D. P. Zipes. 1990. Effects of alpha adrenoceptor stimulation and blockade on early afterdepolarizations induced by cesium in canine cardiac Purkinje fibers. *J. Cardiovasc. Electrophysiol.* 1:31–40.

Kameyama, M., J. Hescheler, F. Hofmann, and W. Trautwein. 1986. Modulation of Ca during the phosphorylation cycle in the guinea pig heart. *Pflügers Arch.* 407:123–128.

Kass, R. S. 1987. Voltage-dependent modulation of cardiac calcium channel current by optical isomers of Bay K 8644: implication for channel gating. *Circ. Res.* 61(suppl. I):1–5.

Kimura, S., A. L. Bassett, H. Xi, and R. J. Myerburg. 1992. Early afterdepolarizations and triggered activity induced by cocaine. *Circulation.* 85:2227–2235.

Kurihara, S., and M. Konishi. 1987. Effects of β-adrenoceptor stimulation on intracellular Ca transients and tension in rat ventricular muscle. *Pflügers Arch.* 409:427–437.

Leblanc, N., and J. R. Hume. 1990. Sodium current-induced release of calcium from cardiac sarcoplasmic reticulum. *Science.* 248:372–376.

LePeuch, C. J., and J. G. Demaille. 1989. Covalent regulation of the cardiac sarcoplasmic reticulum cardiac pump. *Cell Calcium.* 10:397–400.

Luo, C., and Y. Rudy. 1991. A model of the ventricular cardiac action potential: depolarization, repolarization and their interaction. *Circ. Res.* 68:1501–1526.

Luo, C., and Y. Rudy. 1994a. A dynamic model of the cardiac ventricular action potential: I. simulations of ionic currents and concentration changes. *Circ. Res.* 74:1071–1096.

Luo, C., and Y. Rudy. 1994b. A dynamic model of cardiac ventricular action potential: II. Afterdepolarizations, triggered activity and potentiation. *Circ. Res.* 74:1097–1113.

Marban, E., S. W. Robinson, and W. G. Wier. 1986. Mechanisms of arrhythmogenic delayed and early afterdepolarizations in ferret ventricular muscle. *Clin. Invest.* 78:1185–1192.

Markwardt, F., and B. Nilius. 1988. Modulation of calcium channel currents in guinea-pig single ventricular heart cells by the dihydropyridine Bay K 8644. *J. Physiol.* 399:559–575.

Meier, C. F., and B. G. Katzung. 1981. Cesium blockade of delayed outward currents and electrically induced pacemaker activity in mammalian ventricular myocardium. *J. Gen. Physiol.* 77:531–547.

Nattel, S., and M. A. Quantz. 1988. Pharmacological response of quinidine induced early afterdepolarizations in canine cardiac Purkinje fibres: insights into underlying ionic mechanisms. *Cardiovasc. Res.* 22:808–817.

Nunoki, K., V. Florio, and W. A. Catteral. 1989. Activation of purified calcium channels by stoichiometric protein phosphorylation. *Proc. Natl. Acad. Sci. USA.* 86:6816–6820.

Ochi, R., and Y. Kawashima. 1990. Modulation of slow gating process of calcium channels by isoprenaline in guinea-pig ventricular cells. *J. Physiol.* 424:187–204.

Okazaki, O., N. Suda, K. Hongo, M. Konishi, and S. Kurihara. 1990. Modulation of Ca^{2+} transients and contractile properties by β-adrenoceptor stimulation in ferret ventricular muscles. *J. Physiol.* 423:221–240.

Ono, K., T. Kiyosue, and M. Arita. 1989. Isoproterenol, DBcAMP and forskolin inhibit cardiac sodium current. *Am. J. Physiol.* 256:C1131–C1137.

Ono, K., and W. Trautwein. 1991. Potentiation by cyclic GMP of β-adrenergic effect on Ca^{2+} current in guinea-pig ventricular cells. *J. Physiol.* 443:387–404.

Priori, S. G., and P. B. Corr. 1990. Mechanisms underlying early and delayed afterdepolarizations induced by catecholamines. *Am. J. Physiol.* 258: H1796–H1805.

Rasmusson, R. L., J. W. Clark, W. R. Giles, E. F. Shibata, and D. L. Campbell. 1990. A mathematical model of a bullfrog cardiac pacemaker cell. *Am. J. Physiol.* 259:H352–H369.

Rosen, M. R. 1990. The concept of afterdepolarizations. *In* Cardiac Electrophysiology: A Textbook. M. R. Rosen, M. J. Janse, and A. L. Wit, editors. Futura Publishing Company, Inc., Mount Kisco, NY. 267–271.

Rosen, M. R., M. J. Janse, and A. L. Wit. 1990. Cardiac Electrophysiology: A Textbook. M. R. Rosen, M. J. Janse, and A. L. Wit, editors. Futura Publishing Company, Inc. Mount Kisco, NY. 845–876.

Sanguinetti, M. C., D. S. Krafte, and R. S. Kass. 1986. Voltage-dependent modulation of Ca channel current in heart cells by Bay K8644. *J. Gen. Physiol.* 88:369–392.

Shorofsky, S. R., and C. T. January. 1992. L- and T-type Ca^{2+} channels in canine cardiac purkinje cells: single-channel demonstration of L-type Ca^{2+} window current. *Circ. Res.* 70:456–464.

Standen, N. B., and P. R. Stanfield. 1982. A binding-site model for cardiac channel inactivation that depends on calcium entry. *Proc. R. Soc. Lond.* 217:101–110.

Stern, M. D., M. C. Capogrossi, and E. G. Lakatta. 1988. Spontaneous calcium release from the sarcoplasmic reticulum in myocardial cells: mechanisms and consequences. *Cell Calcium.* 9:247–258.

Szabo, G., and A. S. Otero. 1990. G protein mediated regulation of K^+ channels in heart. *Annu. Rev. Physiol.* 52:293–305.

Takamatsu, T., and W. G. Wier. 1989. High temporal resolution video imaging of intracellular calcium. *Annu. Rev. Physiol.* 44:401–423.

Tiaho, F., J. Nargeot, and S. Richard. 1991. Voltage-dependent regulation of L-type cardiac Ca channels by isoproterenol. *Pflügers Arch.* 419:596–602.

Tiaho, F., S. Richard, P. Lory, J. M. Nerbonne, and J. Nargeot. 1990. Cyclic-AMP-dependent phosphorylation modulates the stereospecific activation of cardiac Ca channels by Bay K 8644. *Pflügers Arch.* 417:58–66.

Tourneur, Y., R. Mitra, M. Morad, and O. Rongier. 1987. Activation properties of the inward-rectifying potassium channel on mammalian heart cells. *J. Membr. Biol.* 97:127–135.

Trautwein, W., A. Cavalie, V. Flockerzi, B. F. Hoffman, and D. Pelzer. 1987. Modulation of calcium channel function by phosphorylation in guinea pig ventricular cells and phospholipid bilayer membranes. *Circ. Res.* 61:I-17–I-23.

Tsien, R. W., B. P. Bean, P. Hess, and J. B. Lansman. 1986. Mechanisms of calcium channel modulation by β-adrenergic agents and dihydropyridine calcium agonists. *J. Mol. Cell. Cardiol.* 18:691–710.

Tsien, R. W., W. Giles, and P. Greengard. 1972. Cyclic AMP mediates the effects of adrenaline on cardiac Purkinje fibers. *Nature New Biol.* 240: 181–183.

Tseng, G., R. B. Robinson, and B. F. Hoffman. 1987. Passive properties and membrane currents of canine ventricular myocytes. *J. Gen. Physiol.* 90: 671–701.

Tytgat, J., B. Nilius, J. Vereecke, and E. Carmeliet. 1988. The T-type Ca channel in guinea-pig ventricular myocytes is insensitive to isoproterenol. *Pflügers Arch.* 411:704–706.

Walsh, K. B., T. B. Begenisich, and R. S. Kass. 1988. β-adrenergic modulation in the heart: independent regulation of K and Ca channels. *Pflügers Arch.* 411:232–234.

Walsh, K. B., T. B. Begenisich, and R. S. Kass. 1989. β-adrenergic modulation of cardiac ion channels: differential temperature sensitivity of potassium and calcium currents. *J. Gen. Physiol.* 93:841–854.

Zeng, J., and Y. Rudy. 1994a. Simulation studies of the mechanism of arrhythmogenic early afterdepolarizations in cardiac myocytes. 38th Annual Meeting of The Biophysical Society. *Biophys. J.* 66:322*a*. (Abstr.)

Zeng, J., and Y. Rudy. 1994b. Simulation studies of the rate dependence mechanism of early and delayed afterdepolarizations. *FASEB J.* 6:77*a*. (Abstr.)